Some normal state and superconducting state properties of ultra high purity vanadium

by

Chi-Lan Chang

A Thesis Submitted to the
Graduate Faculty in Partial Fulfillment of the
Requirements for the Degree of
MASTER OF SCIENCE

Department: Materials Science and Engineering
Major: Metallurgy

Iowa State University
Ames, Iowa

1985

TABLE OF CONTENTS

I. INTRODUCTION

In 1908, Kamerlingh Onnes first succeeded in liquifying helium and proceeded to study a number of phenomena in the temperature interval 1 K to 14 K [1]. In 1911, Onnes [2] discovered that the resistivity, ρ, of mercury wires dropped by at least several orders of magnitude in a 0.01 K temperature interval near a critical temperature, T_c, of 4.3 K. Within the error of the experiment, the resistivity dropped to zero and hence, the phenomenon was naturally called superconductivity. Onnes [3] also showed that a critical magnetic field, H_c, would destroy the effect and mapped out a H-T phase boundary separating the superconducting and normal phases.

In 1933, Meissner and Ochsenfeld [4] discovered the so-called "Meissner effect" which demonstrated the reversible nature of the transition. This phenomenon is the complete expulsion of flux from the interior of a solid cylinder situated in a uniform applied field $H_a < H_c$ as the cylinder is cooled toward T = 0 K and it cannot be explained solely on the basis of zero resistivity, but represents a whole new aspect of superconductivity. The Meissner effect showed that a superconductor behaves as a perfect diamagnet and proved that the superconducting state is a stable thermodynamic state. Hence, the Meissner effect led to a thermodynamic description of pure superconductors by Gorter and Casimir [5] and made possible a phenomenological theory, proposed by F. London and H. London [6] of the electromagnetic properties of superconductors. The London theory

predicts that the magnetic induction B does not disappear at the surface of a superconductor, but falls off exponentially with distance into the metal with a characteristic length λ_L, the London penetration depth. Within this theory, λ_L is related to other fundamental parameters by

$$\lambda_L = \left[\frac{m c^2}{4\pi n_s e^2}\right]^{1/2} \qquad (1.1)$$

where m and e are the mass and charge of an electron, c is the speed of light and n_s is the number of electrons per unit volume in the superconducting state. Typically, λ_L = 50 nm for most bulk superconductors.

The basic equations of the London theory are "local" in the sense that they relate the current density and the electromagnetic potential at the same point in space. Pippard [7] in 1953, however, concluded from surface impedance measurements that the current density at a given point in space depends upon the electromagnetic potentials within a region ξ, the Pippard coherence length, about the point in question. The penetration depth determines the static magnetic field variations and the coherence distance determines the degree of locality in the electromagnetic response and the degree of locality of the ground state wave function.

The existence of the coherence length, ξ, and the penetration depth, λ, leads to a natural classification of superconductors into two types in which the primary distinction between the two classes is

based on magnetic behavior and the relative magnitudes of ξ and λ. If $\xi >> \lambda$, the magnetic transition is that of an "ideal" superconductor, showing sharp transition at a magnetic field, H_c (shown by the dashed line in Figure 1), and this class of superconductors is called type-I. If $\xi << \lambda$, on the other hand, the samples exhibit a broad magnetic transition, as shown by the solid line in Figure 1, and this class of superconductors is called type-II and generally is found in alloy systems where electron scattering results in a reduction in the coherence length ξ. Reversible or ideal type-II behavior is difficult to obtain experimentally, because reversibility is especially sensitive to defects and unwanted impurities.

Type-I superconductors are described by the nonlocal Pippard theory. In this class, are the physically soft (hence, the term "soft superconductors") low melting point materials, such as lead, tin, indium, mercury and many of the pure metal superconductors, and low concentration alloys with long electronic mean free paths. From the microscopic point of view, the properties of type-I superconductors are well explained by the theory of Bardeen et al. [8], the BCS theory. The BCS theory was able to account for the specific heat, the acoustic attenuation, the infrared absorption, the tunneling effects, etc.

Type-II superconductors in the short mean free path limit are described by the London theory in small magnetic fields and are usually characterized by $\lambda >> \xi$. In this category are most chemical compounds, such as Nb_3Sn, V_3Ga, Nb(Ta), and the pure metals niobium and vanadium which are physically hard (hence, the term "hard superconductors"),

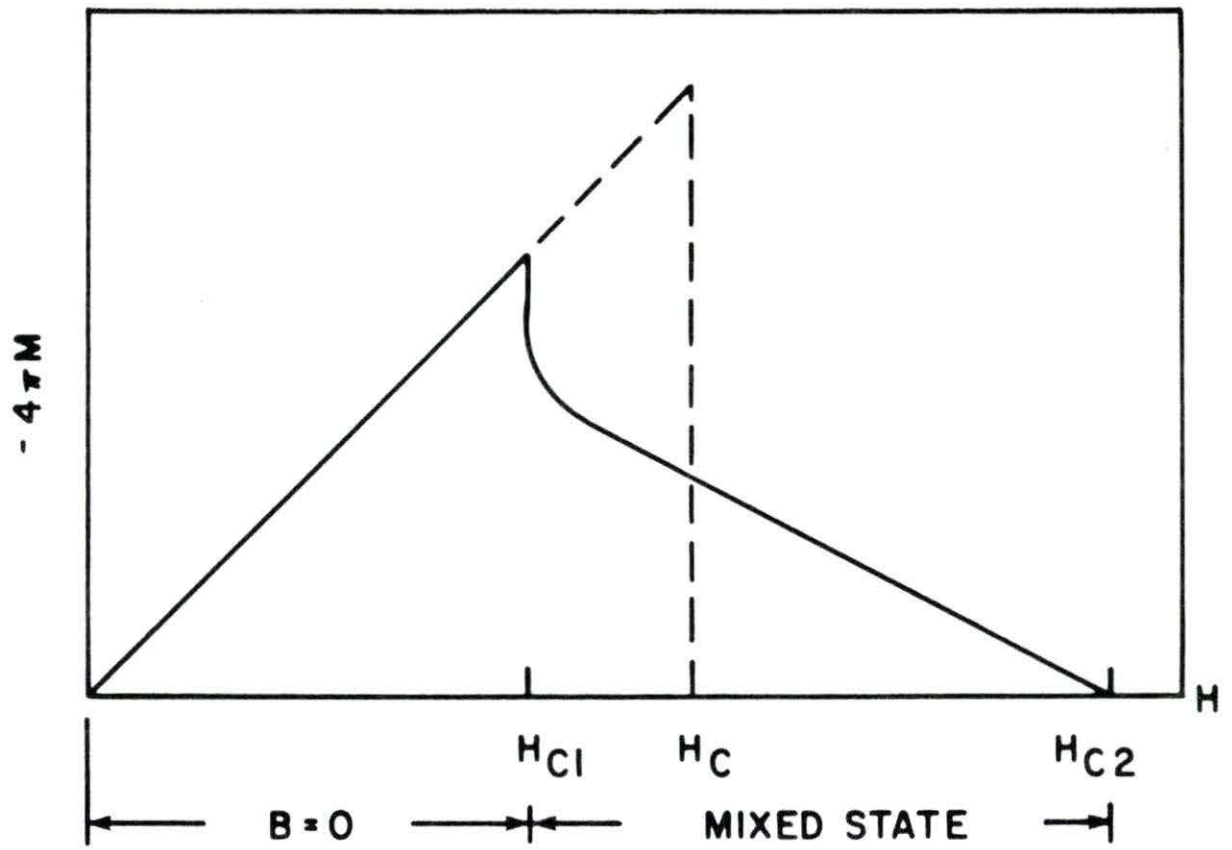

Figure 1. Magnetization curve for an ideal type-II superconductor

and have high melting points. This class of superconductors was first investigated by Shubnikov et al. [9] in 1937 and has become increasingly important in the past twenty years.

A macroscopic cylinder of an ideal type-II superconductor placed in a field H parallel to its axis exhibits the bulk properties shown in Figures 1 and 2. There are four regions of interest, depending on the value of the external field. For $H < H_{c1}$, there is complete exclusion of the magnetic induction from the sample (the Meissner effect) (see Figure 2). For $H_{c1} < H < H_{c2}$, flux penetrates the sample in a nonuniform manner, but the magnetic induction remains smaller than the applied field. In this region, a new state appears in which a triangular lattice of quantized flux-enclosing supercurrent vortices (or filaments) is formed, the magnetic flux contained within vortex cell being equal to the magnetic flux quantum ($\sim 2 \times 10^{-7}$ gauss cm^2). This state is commonly called the "mixed state", the "vortex state", or the "Shubnikov state". For $H_{c2} < H < H_{c3}$, the bulk of the specimen becomes normal, but a superconducting sheath of thickness ξ exists on the surface of the metal. For $H > H_{c3}$, the entire sample is in the normal state.

The characteristics of superconductivity in Nb and V have attracted considerable interest because the metals (and possibly Tc and La) are the only known elemental superconductors which are type-II for all temperatures below their respective transition temperatures. Both Nb and V have a crystal lattice of body-centered cubic. The superconducting properties of the elemental type-II superconductor vanadium in fairly

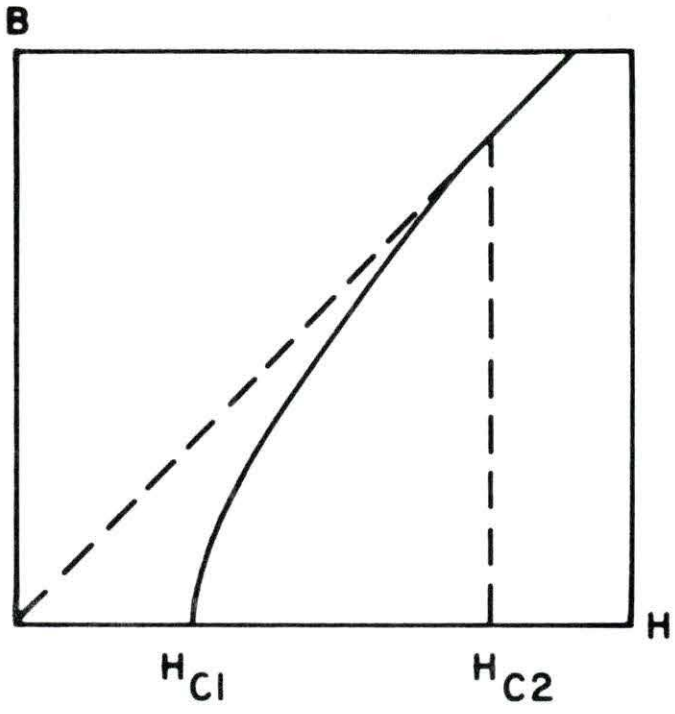

Figure 2. Schematic variation of the induction B versus the applied field H in a type-II superconductor

pure form (resistivity ratio $\Gamma = \rho(273\ K)/\rho(4\ K) \approx 130$) have been previously reported [10, 11]. With the availability of a higher purity vanadium ($\Gamma_{4.2} \approx 190$), it was felt that further study of the magnetic properties of this material in the superconducting state would be worthwhile, since such experimental data would be useful in an examination of the validity of "clean-limit" theories of type-II superconductivity.

In addition, the theoretical work by Rietschel and Winter [12] and Rietschel [13] indicates that spin fluctuations are present in vanadium. Not only the specific heat coefficient γ, but the thermodynamic critical field $H_c(0)$ and the heat-capacity jump ΔC are also strongly affected by spin fluctuations (more details are presented in Chapter II). In the past few years, Gschneidner and co-workers have found that the application of high magnetic fields can quench spin fluctuations (e.g., see Ref. [14]). Thus, another reason for investigating the magnetic field dependence of the heat capacity of vanadium is to see if the spin fluctuations can be quenched in vanadium. The temperature dependence of the magnetic susceptibility may also indicate the presence of spin fluctuation [14, 15].

In this work, the studies are emphasized on the low temperature heat capacity, electrical resistivity, resistive transition and magnetic susceptibility measurements. These measurements were combined to obtain a set of superconducting and normal state material parameters like $H_c(0)$ (thermodynamic critical field at 0 K), $H_{c2}(0)$ (upper critical magnetic field at 0 K), ΔC (jump in the heat capacity

at T_c), $2\Delta(0)/kT$ (reduced gap parameter), D(t) (deviation function), λ (electron-phonon coupling parameter), N(0) (electronic density of states at Fermi surface at 0 K), κ_0, κ (generalized Ginzburg-Landau parameters), S (area of the Fermi surface in k-space), $\lambda_L(0)$ (London penetration depth), ξ_0 (intrinsic coherence length), ℓ (electron mean free path) and V_F (average Fermi velocity). The results are compared to the BCS predictions and the theory for weak-coupling type-II superconductor. The results suggest that vanadium is weak-coupling clean type-II superconductor.

II. BACKGROUND THEORY

A. Electrical Resistivity

For a conductor of uniform cross-sectional area, A, and length, ℓ, in which a current, I, flows, a voltage, V, between its ends will be developed and is given by the relation

$$V = \frac{I \rho \ell}{A} = IR \tag{2.1}$$

where $\rho = RA/\ell$ is the electrical resistivity which is characteristic of a given conductor and R is the electrical resistance. Eq. (2.1) is an expression of Ohm's law.

The electrical resistivity, ρ, of a metal in general decreases with temperature in a uniform manner. Resistivity for a metal may be defined by

$$\rho = \frac{m^*}{N e^2} \frac{1}{\tau} \tag{2.2}$$

where m^* is the effective mass of an electron in the material, N is the concentration of conduction electrons, e is the electronic charge, and τ is the scattering time, or time between scattering events. The resistivity is thus proportional to the probability that an electron will scatter per unit time.

There are two causes for electron scattering events: (i) lattice vibrations (phonons), and (ii) lattice imperfections and impurities.

The resistivity can be divided into two parts, one for each cause of electron scattering, commonly known as Matthiessen's rule:

$$\rho(T) = \rho_r + \rho_i(T) \tag{2.3}$$

where ρ_r is the residual resistivity determined at the absolute zero temperature, and arises from the scattering of conduction electrons by impurities, defects or strains in the metal lattice. $\rho_i(T)$ is the intrinsic or ideal resistivity contributed by the phonons, which is temperature dependent; at low temperatures, the phonons should be "frozen out", that is, the lattice vibration amplitudes should be very small so the low temperature resistivity should be approximately equal to ρ_r and is temperature independent. The value of $\Gamma_{4.2} \approx \rho(300\ K)/\rho(4.2\ K)$ is thus a measure of the relative amount of impurities and imperfections in a given sample relative to other samples of the same material: a high value of $\Gamma_{4.2}$ indicates that only a few impurities and defects are present.

B. Heat Capacity and Superconductivity

As mentioned in Gopal's book [16], for a non-magnetic conductor, the observed heat capacity is of the form

$$C = C_e + C_{latt} \tag{2.4}$$

where C_e and C_{latt} are the electronic and lattice heat capacities,

respectively. The C_e term varies linearly with temperature as given by

$$C_e = \gamma T \tag{2.5}$$

where γ is called the electronic specific heat constant. In the free electron model, the γ is related to the density of state at the Fermi energy at 0 K (N(0)) and the relationship is given as

$$\gamma = \frac{2\,\pi^2\,k^2\,N(0)}{3} \tag{2.6}$$

where k is the Boltzmann constant. Note that the electronic term measures merely an averaged density of state at the Fermi surface. The electron-phonon interaction will enhance γ by a factor of $(1 + \lambda_{ep})$, where λ_{ep} is called the electron-phonon coupling parameter. Now, γ is related to N(0) as

$$\gamma = \frac{2\,\pi^2\,k^2\,N(0)\,(1 + \lambda_{ep})}{3} \quad . \tag{2.7}$$

At low temperature for which $T \leq \theta_D/50$, the lattice contribution to the heat capacity (C_{latt}) in terms of the Debye model can be expressed as

$$C_{latt} = \beta\,T^3$$

$$= 1.944 \times 10^6\ \frac{T^3}{\theta_D{}^3} \tag{2.8}$$

where θ_D is the Debye temperature which is characteristic of the phonon spectrum and the units of C_{latt} are in mJ/g-atom-K.

Substituting Eqs. (2.5) and (2.8) into Eq. (2.4), and dividing through by T, we obtained the expression

$$\frac{C}{T} = \gamma + \beta T^2 . \qquad (2.9)$$

Thus, a plot of C/T vs. T^2 will give a straight line, and the intercept at 0 K gives the γ value, while the slope of the line gives the β value from which θ_D can be calculated.

The above discussion applies to the normal conductors. When a metal becomes superconducting at temperatures below T_c, the lattice heat capacity is assumed unchanged since no structural changes are involved, but the electronic heat capacity is altered. The electronic heat capacity in the superconducting state (C_{es}) can be determined from the relation

$$C_{es} = C_s - C_n + \gamma T \qquad (2.10)$$

where s and n indicate the superconducting and normal states, respectively. Experimentally, it has been found that C_{es} varies as

$$\frac{C_{es}}{\gamma T_c} = a \exp\left(- b \frac{T_c}{T}\right) . \qquad (2.11)$$

The experimental variation of the heat capacity indicates the

existence of an energy, 2Δ, separating the normal and superconducting electrons.

If the difference of lattice specific heat between superconducting and normal state is negligible, the Bardeen-Cooper-Schrieffer (BCS) theory predicts that

$$\frac{C_{es}}{\gamma T_c} = 8.5 \exp \frac{-1.44\ T_c}{T} \qquad \text{for } 2.5 < \frac{T_c}{T} < 6$$

$$= 26 \exp \frac{-1.62\ T_c}{T} \qquad \text{for } 7 < \frac{T_c}{T} < 12 \tag{2.12}$$

where the energy gap, 2Δ, is related to T_c by means of the relation

$$2\Delta = 3.52\ k\ T_c\ . \tag{2.13}$$

Another prediction of the BCS theory is that the jump in heat capacity at T_c ($\Delta C(T_c)$) is given as

$$\begin{aligned} \Delta C(T_c) &= C_s(T_c) - C_n(T_c) \\ &= C_{es}(T_c) - C_{en}(T_c) \\ &= 1.43\ \gamma\ T_c\ . \end{aligned} \tag{2.14}$$

The thermodynamic functions derived from the heat capacity results are given below. The entropy, S, at any temperature, T, may be uniquely expressed as

$$S_i(T) = \int_0^T \frac{C_i(T)}{T}\, dT \qquad (2.15)$$

where i is s or n for superconducting or normal state, respectively. At $T = T_c$, $S_s = S_n$, i.e., the entropy values are equal for both states. The Gibbs free energy at any temperature can be expressed as

$$G_i(T) = U_i + (PV)_i - \int_0^T S_i(T)\, dT \qquad (2.16)$$

where U is the internal energy and PV is the product of the pressure and volume.

In a magnetic field, H, the Gibbs free energy in the superconducting state ($G_s(T, H)$) is given as

$$G_s(T, H) = G_s(T) - \frac{1}{2} MH \qquad (2.17)$$

where $G_s(T)$ denoted the superconducting Gibbs free energy in zero field and M is the induced moment given as

$$M = - \frac{H V}{4 \pi} \qquad (2.18)$$

where V is the molar volume. On the equilibrium curve, i.e., $H = H_c$, the free energies of both states must be equal and so

$$G_n(T, H_c) = G_s(T, H_c)$$

$$= G_s(T) - \frac{1}{2} M H_c(T)$$

$$= G_s(T) + \frac{V}{8\pi} [H_c(T)]^2 \qquad (2.19a)$$

or

$$G_n(T, H_c) - G_s(T) = \frac{V}{8\pi} [H_c(T)]^2 \qquad (2.19b)$$

where $H_c(T)$ is called the critical thermodynamic field. From Eq. (2.16) and with the assumption that the first two terms have the same values in the normal and superconducting states, Eq. (2.19b) becomes

$$G_n(T, H_c) - G_s(T) = - \int_o^T S_n(T, H_c)\, dT + \int_o^T S_s(T)\, dT$$

$$= \int_o^{T_c^*} [S_n(T, H_c) - S_s(T)]\, dt \quad . \qquad (2.19c)$$

By substituting the right-hand side of Eq. (2.19b) for the left-hand side of Eq. (2.19c), we obtained

$$= \frac{V}{8\pi} [H_c(T)]^2 \quad .$$

The values of the $H_c(T)$ are related to the T empirically as

$$H_c(T) = H_c(0) [1 - t^2] \qquad (2.20)$$

where $t \equiv T/T_c$.

The BCS theory explains the behavior of type-I superconductors quite well and the above thermodynamic relations are obeyed. For a type-II superconductor, the superconductivity is destroyed at a much higher field, called the upper critical field, $H_{c2}(T)$. The $H_{c2}(T)$ is related to the $H_c(T)$ in the theory proposed by Maki [17]. He introduced the parameters κ_1 and κ_2 defined as

$$\kappa_1 = \frac{H_{c2}(T)}{\sqrt{2}\, H_c(T)} \tag{2.21}$$

$$\left[\frac{dM}{dH}\right]_{H=H_{c2}} = \frac{1}{4\pi\, \beta_A(2\,\kappa_2^2 - 1)} \tag{2.22}$$

and the Ginsburg-Landau parameter, κ, is defined as

$$\kappa = \kappa_1(T_c) = \kappa_2(T_c) \tag{2.23}$$

where $(dM/dH)_{H=H_{c2}}$ is the slope of the magnetization curve at $H_{c2}(T_H)$ and β_A is a constant (1.159 for the more favorable triangular lattice [18]). According to Goodman [19], the slope of the magnetization curve at $H_{c2}(T_H)$, $(dM/dH)_{H=H_{c2}}$, can be obtained from the relation

$$\frac{\Delta C(H)}{V\, T_H} = \left[\frac{dM}{dH}\right]_{H=H_{c2}} \left[\frac{dH_{c2}}{dT}\right]^2_{T=T_H} \tag{2.24}$$

where $\Delta C(H)$ is the jump in heat capacity in field H and T_H is the superconducting temperature in that field. From Eqs. (2.22) and (2.24), the values of $\kappa_2(T)$ can be calculated.

As reported by Goodman [20], the Ginzburg-Landau parameter, κ, can be expressed as a sum of two terms

$$\kappa = \kappa_0 + \kappa_\ell \tag{2.25}$$

where κ_ℓ depends on the electron mean free path ℓ. The term κ_ℓ is expressed in terms of measurable quantities as

$$\kappa_\ell = 7.53 \times 10^3 \, \gamma^{1/2} \, \rho_r \tag{2.26}$$

where γ is in ergs-cm^{-3}-K^{-2} and ρ_r, the residual resistivity, in Ω cm.

Gor'kov [21] showed that the parameter κ_0 may be written as

$$\kappa_0 = 0.96 \, \frac{\lambda_L(0)}{\xi_0} \quad , \tag{2.27}$$

and Hake [22] reported that the intrinsic coherence length, ξ_0, and the London penetration depth, $\lambda_L(0)$, can be determined from the relations

$$\xi_0 = \frac{0.18 \, k \, S}{12 \, \pi \, \gamma \, T_c} \tag{2.28}$$

and

$$\lambda_L(0) = \frac{3\ h\ \pi^{1/2}\ \gamma^{1/2}}{e\ k\ S} \tag{2.29}$$

where e is the electronic charge in emu, S is the area of the Fermi surface in k-space excluding zone boundaries, h is Planck's constant and all quantities are in cgs units. Substituting Eqs (2.28) and (2.29) into Eq. (2.27), the parameter κ_0 can be expressed as

$$\kappa_0 = 1069\ \frac{h\ \gamma^{3/2}\ T_c}{e\ k^2\ S^2}$$

$$= 1.61 \times 10^{24}\ \frac{T_c\ \gamma^{3/2}}{n^{4/3}}\ \left(\frac{S}{S_F}\right)^{-2} \tag{2.30}$$

where n is the number of valence electrons per cm^3 (for vanadium, $n = 3.61 \times 10^{23}\ cm^{-3}$) and S_F is the area of the Fermi surface for a free-electron gas of density n, and $S_F = 4\pi(3\pi^2 n)^{2/3}$. Then, S can be obtained from Eq. (2.30). The electron mean free path, ℓ, and the average Fermi velocity, V_F, as reported by Fawcett [23], are given by

$$\ell = \frac{6\ \pi^2\ h}{e^2\ \rho_r\ S} \tag{2.31}$$

and

$$V_F = \frac{6\ h\ \gamma}{k^2\ S}\ . \tag{2.32}$$

C. Magnetic Susceptibility

The magnetic susceptibility of a material is defined as the ratio of the magnetization, M, of the materials over the applied magnetic field, H. If the susceptibility is small, the applied field is relatively unchanged by the magnetization and the relationship

$$\chi = \frac{M}{H} \tag{2.33}$$

holds.

The potential energy of the material in a magnetic field is likewise given by

$$U = \frac{m}{2} MH \tag{2.34}$$

where U is the potential energy and m is the mass of the sample. Using the definition for the susceptibility given by Eq. (2.33), Eq. (2.34) becomes

$$U = - (m \frac{\chi}{2}) H^2 . \tag{2.35}$$

The Faraday method for determining the magnetic susceptibility measures the force, F, on a sample placed in a nonhomogeneous magnetic field. This force can be derived from the potential energy equation by taking the first derivative with respect to the direction of the force, or

$$F_z = -\frac{dU}{dz} = \left(m \frac{\chi}{2}\right) \frac{d(H^2)}{dz} \quad . \tag{2.36}$$

When cgs units are used, F is expressed in dynes.

If the magnetic field is unidirectional (i.e., $H_y = H_z = 0$, or H is directed only along the x direction) in the volume of the sample, then

$$F_z = \left(\frac{m\chi}{2}\right) \frac{d(H_x^2)}{dz} \quad . \tag{2.37}$$

The force measured on a balance is typically expressed in terms of mass, so the result is

$$F_z = \Delta(mg) = g(\Delta m) = \left(\frac{m\chi}{2}\right) \frac{d(H_x^2)}{dz} \tag{2.38}$$

where g is the earth's gravitational constant (= 980 $cm \cdot sec^{-2}$) and Δm is the apparent mass change on the balance between the time the magnetic field is present ($H \neq 0$) and zero field. With a material of unknown susceptibility (in terms of electromagnetic units per gram (emu/g)), Eq. (2.38) is rearranged to give

$$\chi = \frac{2\ g\ \Delta m}{m \dfrac{d(H_x^2)}{dz}} \quad . \tag{2.39}$$

The gravitational constant and $d(H_x^2)/dz$ will remain constant of the equipment when it is operated under standardized conditions. Thus, by using a sample of known weight, the gram susceptibility can be determined by measuring the apparent change in mass when the magnetic field is alternately turned on and off. In practice, the apparent mass change must also take into consideration the susceptibility of the sample holder. This can be treated as an additive constant to either the susceptibility or the apparent mass change, i.e.,

$$\chi = \left[\frac{2\ g\ \Delta m}{\frac{d(H_x^2)}{dz}} - \chi_{holder}\right]/m \qquad (2.40a)$$

or

$$\chi = \frac{2\ g(\Delta m - \Delta m_{holder})}{m\ \frac{d(H_x^2)}{dz}} \quad . \qquad (2.40b)$$

For this study, it was found to be easier to measure the apparent mass change of the holder at various standardized field settings and subtract its mass change from the total measured mass change to obtain the apparent mass change of the sample.

D. Role of Spin Fluctuations in Vanadium

From the theoretical work by Rietschel [13], it has recently been argued that spin fluctuations are widespread and important as a pair-breaking mechanism. The specific heat coefficient, γ, the

thermodynamic critical field, $H_c(0)$, and the heat capacity jump, ΔC, are defined as

$$\gamma = \frac{2\pi^2 k^2 N(0) (1 + \lambda)}{3} \tag{2.41}$$

$$H_c^2(0) = \frac{2\pi \gamma T_c^2}{1 - \alpha} \tag{2.42}$$

$$\Delta C(T_c) = \frac{2 \gamma T_c (1 + \beta)^2}{1 - \alpha} \tag{2.43}$$

where λ is the electron mass enhancement factor which can be split into an electron-phonon part and a spin fluctuation part,

$$\lambda = \lambda_{ep} + \lambda_{spin} \quad . \tag{2.44}$$

The quantities α and β are related to $D(t)$ through

$$\alpha = \frac{d\, D(t)}{d\, (t^2)} \Bigg|_{t=0} \tag{2.45}$$

$$\beta = - \frac{d\, D(t)}{d\, (t^2)} \Bigg|_{t=1} \tag{2.46}$$

For the electron mass enhancement factor, λ, one has

$$\lambda_{ep} = 2 \int_0^\infty d\omega \, \frac{\alpha^2 F(\omega)}{\omega} \tag{2.47}$$

$$\lambda_{spin} = 2 \int_0^\infty d\omega \, \frac{P(\omega)}{\omega} \tag{2.48}$$

where $\alpha^2 F(\omega)$ is the Eliashberg function and $P(\omega)$ is the spectral weight function of the spin fluctuation.

Since α and β are small quantities ($\lesssim 10^{-1}$) and in addition, almost insensitive to spin fluctuation, then one obtains

$$\gamma \sim (1 + \lambda) \tag{2.49}$$

$$H_c(0) \sim (1 + \lambda)^{1/2} \tag{2.50}$$

$$\Delta C(T_c) \sim (1 + \lambda) \quad . \tag{2.51}$$

III. EXPERIMENTAL PROCEDURE

A. Sample Preparation

The vanadium metal used in this study was obtained from Mr. F. A. Schmidt at the Ames Laboratory, and was prepared by an electrotransport process in a vacuum of 10^{-8} torr. The vanadium specimen was cylindrical in shape with a diameter of about 0.15 in. and a length of 1.5 in.

B. Electrical Resistivity Measurements

The ac electrical resistivity of vanadium was measured using the four-probe technique over the temperature range 4 to 300 K. The sample was cut into a rectangular rod shape by a diamond saw. Four 0.002 in. diameter platinum wires were fixed to points on circumference of the top of the sample with spots of silver epoxy. These leads were then soldered to the copper posts of the resistivity cryostat, which were connected to the electronics outside the helium dewar. A small alternating current, typically 2 mA peak to peak, was sent through two adjacent wires, and the voltage across the other pair was measured using a Princeton Applied Research (PAR) model 124A lock-in amplifier. The sample voltage was amplified using a PAR model 116 differential pre-amplifier to increase the sample voltage by a factor of 100 before going to the lock-in amplifier. The current was determined by measuring the voltage across a standard 1 mΩ resistor with the lock-in amplifier. By admitting a small pressure (about

10 militorr) of helium exchange gas to the vacuum can surrounding the sample holder, the temperature of the sample was allowed to decrease slowly (approximately 100 K/hour) to that of surrounding bath, and measurements were taken from room temperature to just below the superconducting transition temperature. A calibrated platinum thermometer was used in the 30 to 300 K temperature range, and a calibrated carbon glass thermometer was used below 30 K.

The method of van der Pauw [24] was used to determine the specific resistivity values from the measured voltages; the use of this method is outlined in Chapter IV. The sample thickness used in calculations was measured with vernier calipers. Because the sample current was essentially constant over the entire temperature range, the value of $\rho(T)/\rho(300\ K)$ was the sample voltage at temperature T divided by the sample voltage at room temperature.

C. Upper Critical Field Measurement

The magnetic susceptibility of pure vanadium was measured over the temperature interval of 1.5 to 300 K. Measurement was made on a microcomputer-controlled Faraday magnetic susceptibility apparatus.

The magnetic field is produced by a Harvey-Wells water-cooled electromagnet powered by a solid-state power supply capable of providing 100 volts dc at 200 amperes, and produces magnetic fields up to 2.7 tesla.

One important aspect of the Faraday method is the preparation of the magnetic field to give an accurate field constant, $d(H_x^2)/dz$. This

field constant must change as little as possible over the volume where the sample is located.

An all-glass liquid helium dewar manufactured by Pope Scientific Company is used as the cryostat. This dewar has a liquid nitrogen jacket along with the vacuum jacket around the He reservoir and a taped tailstock which fits between the magnet pole pieces. The vacuum jacket is evacuated using a mechanical rotary vacuum pump and the inner jacket can be isolated by closing a ground-glass stopcock. A Stokes pump is used to pump on the liquid helium reservoir to obtain temperatures as low as 1.5 K.

The sample is placed in a separate vacuum chamber, the lower part of which is within the liquid He reservoir. In the upper part of the sample chamber, there are ports for evacuating the sample chamber and an entry valve for admitting helium gas into the chamber. The details of the cryogenics and the sample holder were described in the thesis of R. J. Stierman [25].

Temperature was measured using a set of three resistance thermometers (RTs): a platinum resistance thermometer (PRT), a germanium resistance thermometer (GRT), and a carbon resistance thermometer (CRT). The PRT has a linear response of resistance versus temperature from 40 K up to 300 K. Temperatures below 40 K require the use of GRT and CRT. The CRT has a much smaller magnetoresistance than the GRT, which means it is usable in magnetic fields. The PRT does not have a noticeable magnetoresistance and no corrections need to

be made for magnetic fields. Therefore, between GRT-CRT combination below 45 K and the PRT above 45 K, the temperature can be determined at any time for the entire 1.5 to 300 K range.

Thermal contact is made between the sample holder and the RTs through the admittance of a liberal amount of He gas into the sample chamber as an exchange medium. Before backfilling with exchange gas, the sample chamber is evacuated by a mechanical rotary pump to a vacuum of 15 millitorr or better. Since the volume of the sample holder is constant and the pressure throughout the sample chamber (at least 100 millitorr at all temperatures) is uniform, no buoyancy effects should arise which would have a noticeable effect on the balance during the course of a measurement.

The RTs are wired in series along with two $\pm$ 0.005% standard resistances of 100 Ω and 1000 Ω. Wires are attached to measure all resistors via a four-wire method, i.e., measure the voltage drop across each resistor with Data Precision model 3500 digital voltmeter (DVM). By comparing the voltage drop across each of the RTs and standards, the resistance of each RT is determined.

The force is measured using a Cahn model RH recording electrobalance. This unit has a resolution of 2 micrograms and a maximum load of 100 grams. The control unit has a voltage output that is proportional to the force on the balance arms and was calibrated so 1 volt output equals 1 gram weight. The output is measured on the DVM used to measure the RTs.

A double-helical wound heater made of number 34 manganin wire is used to maintain temperature below 300 K. The details of heater assembly and computer controlled apparatus were described in Stierman's thesis [25].

Dr. D. K. Finnemore's resistivity apparatus was used to measure the superconducting transition temperature as functions of magnetic field from 0 to 0.7 tesla and temperature from 1.3 K to 20 K. The dewar system (Figure 3) used in this experiment is a standard design for work in magnetic field at temperatures between 1 and 20 K. Both the liquid nitrogen and liquid helium metal dewars were built in the Ames Laboratory shops. Magnetic fields were generated by a 7500 Oe liquid nitrogen cooled compensated solenoid which surrounded the tail of the helium dewar. J. R. Hopkins' thesis [26] described the details of the experimental apparatus. The magnitude of the field (as a function of current in the solenoid) was determined by nuclear magnetic resonance. The proton resonance in glycerin was measured and yielded a value of 152.45 $\pm$ 0.02 Oe/amp for the fields used.

Temperature control in the sample region was accomplished by pumping on the helium bath through a manostat for temperatures below 4.2 K. Before pumping the bath for temperatures below 4.2 K, the vacuum space in the heat leak chamber, as well as the heat leak chamber itself, was subjected to an over pressure of helium gas in order to condense liquid helium around the sample. During the pumping operation, these regions were kept at the same pressure as the surrounding bath using external connections.

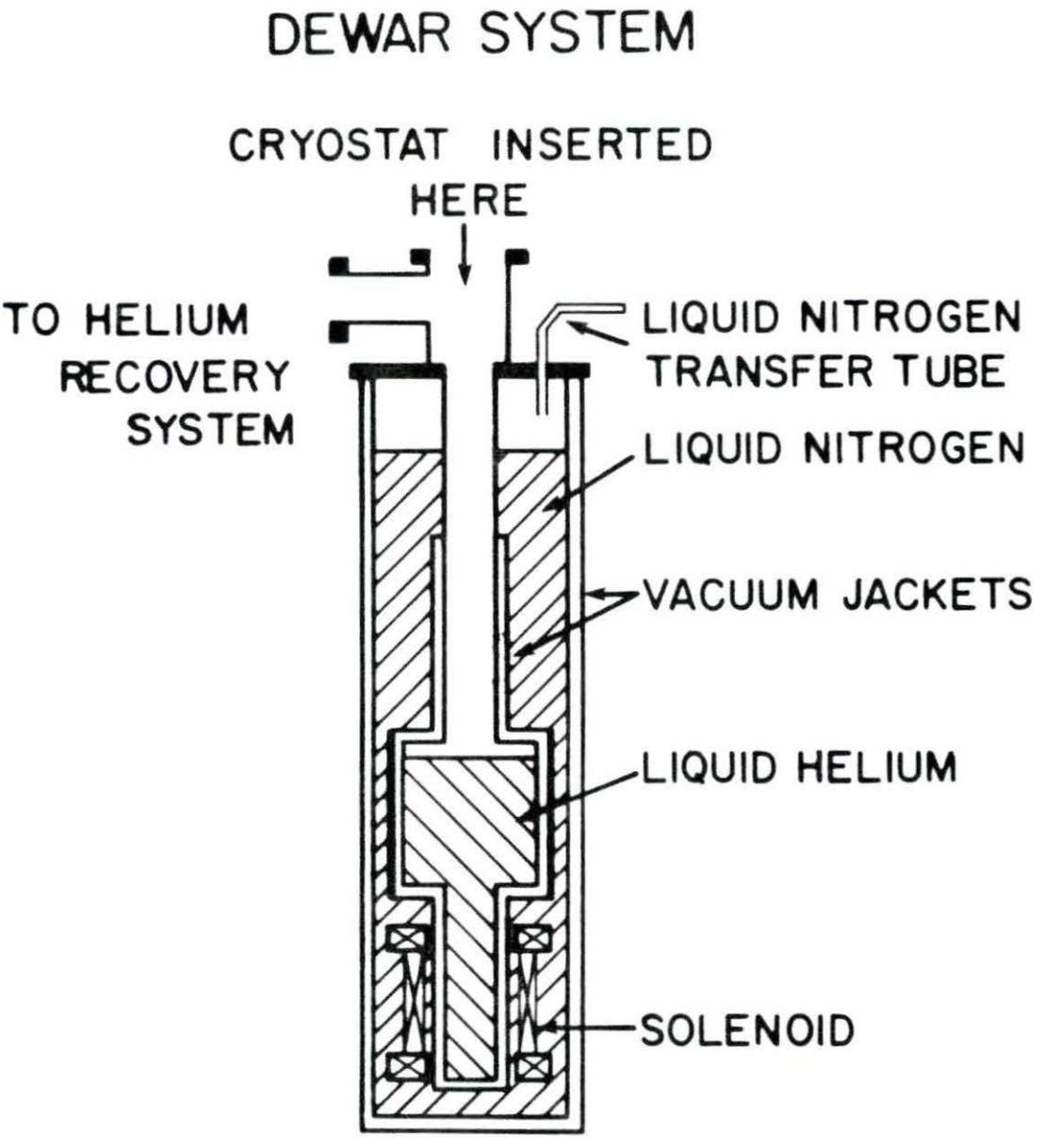

Figure 3. The dewar system

With temperatures greater than 4.2 K, a manganin heater astatically wound around the outside of the inner portion of the heat leak chamber was used to elevate the temperature slowly by increasing a slight heater current (0.01 - 1 mA).

A carbon-glass resistance thermometer was used in this experiment to measure the temperature. The desired bath temperature was obtained by adjusting the pumping speed on the helium bath in conjunction with an electronic temperature control system.

For temperatures higher than 4.2 K, several fixed magnetic fields were used to measure the superconducting transition temperatures. The superconducting transition temperature was obtained from the point at which the normal state resistance dropped 50% of the total change in resistance at T_c for a given magnetic field. It was found that the superconducting transition temperature was lower at the higher magnetic field. For temperatures lower than 4.2 K, a fixed temperature was obtained by reducing the vapor pressure over the liquid helium pot. In this case, the critical field at a given temperature was obtained from the 50% drop of the normal state resistance at T_c. The superconducting transition of vanadium tends to broaden in high fields, which might introduce some systematic errors.

D. Calorimetry

The low temperature calorimeter was constructed in 1977-1978 by Dr. U. Atzmony and Mr. J. O. Moorman. The initial germanium resistance thermometer was replaced by a new one in 1981 and the new GRT was

calibrated as described in the thesis of Y.-C. S. Yeh [27].

The calorimeter was designed for accurate measurements of small samples in the temperature interval of 1.4 to 20 K. A superconducting solenoid made of Nb_3Sn by Intermagnetics Corporation was used to generate magnetic fields up to 10 tesla. This would enable us to study the heat capacity of superconductors in magnetic fields. Because the superconducting transition temperature is suppressed by the magnetic field, the normal state properties, such as γ and θ_D, are more accessible, and the field dependence of T_c and the $H_{c2}(T)$ can be determined.

The vanadium sample was prepared for calorimetry by electropolishing, rinsing with acetone, and then drying in air. The sample was weighed, then a few mg of Apiezon N grease were added to form a bond between the sample and the sample holder of the calorimeter.

The calorimeter was of the isolation heat-pulse type and it consisted of three parts: the cryogenic system, the heater circuit and the temperature measurement circuit. The first part consists of the dewars to cool the system and the sample chamber. The outermost dewar contained liquid nitrogen which provided a 77 K environment and together with the vacuum space, maintained by a mechanical fore pump, act as shields for the inner helium dewar which serves as the liquid helium reservoir.

The calorimeter, as shown in Figure 4, was suspended from the top of the dewar assembly by two stainless steel tubes which also serve as the pumping lines for the helium pot and the sample chamber. The helium pot was pumped by a Microvac Stokes pump while vacuum ($<10^{-7}$ torr)

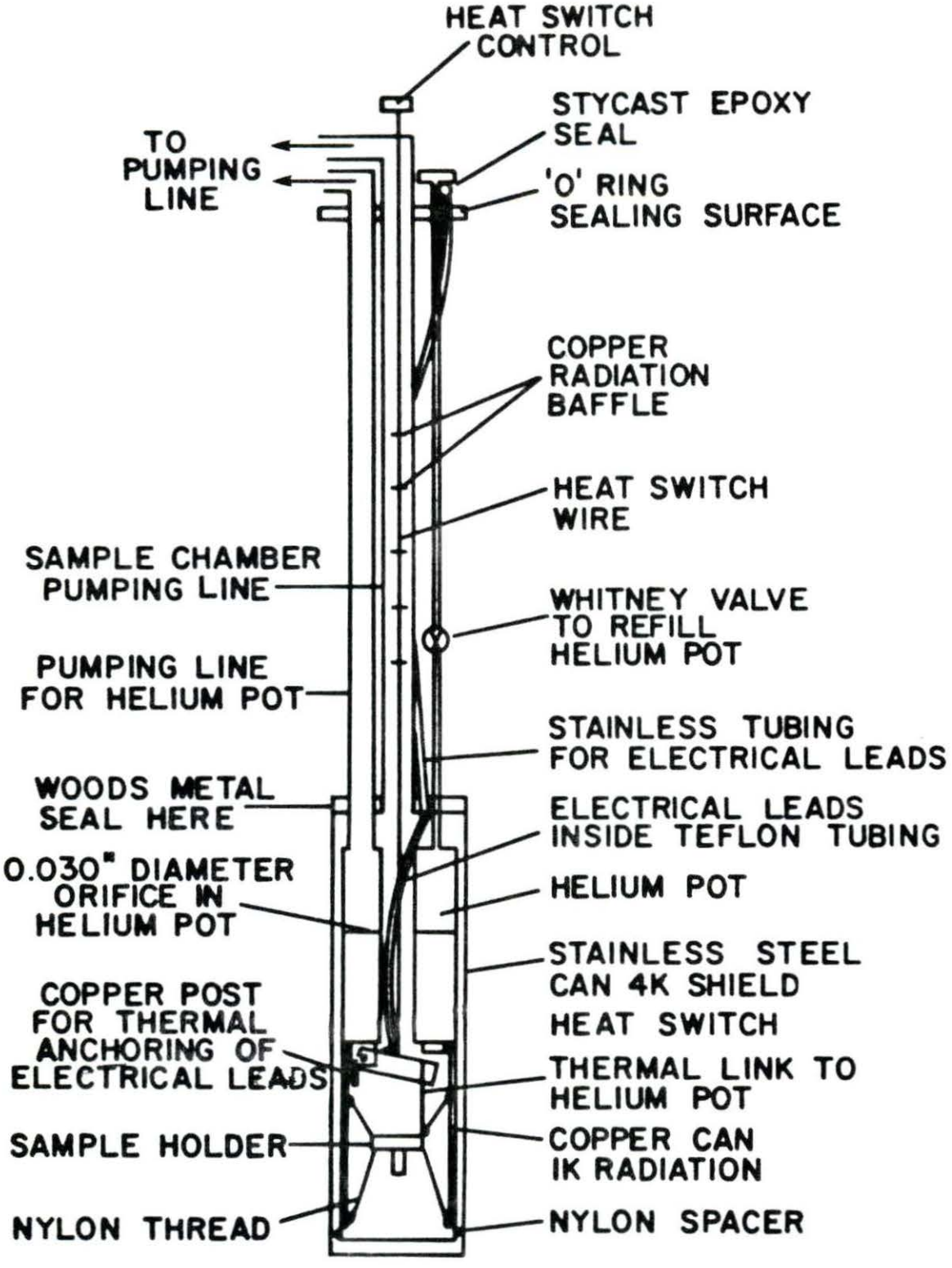

Figure 4. The low temperature calorimeter

in the sample chamber is maintained by an oil diffusion pump backed with a mechanical fore pump. The helium pot and the sample chamber sit inside a stainless steel can which is directly immersed in liquid helium and thus, functions as the 4 K shield. This 4 K shield was joined to the calorimeter by Wood's metal seal and the system was checked for vacuum leaks. Only after a good vacuum was achieved in the sample chamber, the liquid nitrogen and the liquid helium were transferred. A Whitney valve was used to allow liquid helium to flow from the reservoir through a thin-walled stainless steel tube into the pot. By reducing the vapor pressure over the liquid helium in the pot, a temperature of approximately 1.4 K can be achieved. A 0.03 in. diameter orifice located part way down the pot was used to control the flow of the helium superfluid below the λ-point at 2.2 K.

In the sample chamber, a mechanical heat switch was used to control the thermal contact of the addenda and sample to the inner pot. In the closed position, the addenda and sample were cooled down to the temperature of the inner pot. In the open position, the addenda and sample were isolated and they could be warmed by a heater. The sample chamber is shown in detail in Figure 5. In the sample holder, a sample is clamped between two copper discs which were tightened by a screw, and the GRT and the capacitance thermometer (CT) were sitting on the top disc. In this holder, the sample sat on a copper foil container and the GRT was fastened underneath the container.

The second part of the calorimeter was the heater circuit. A length of 1 mil-diameter 92% Pt-8% W was used as the heater wire due

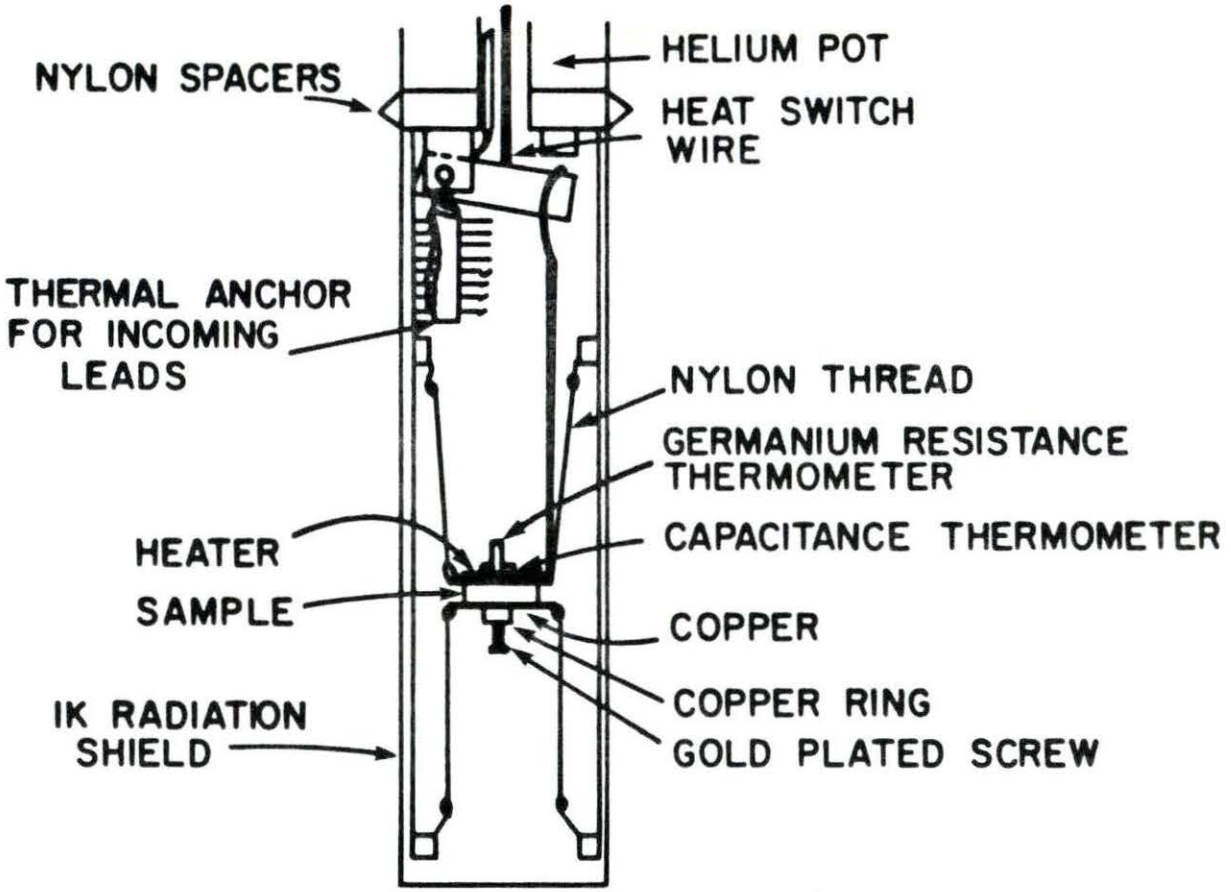

Figure 5. The view of the sample chamber in the calorimeter

to its strength, high resistance and low temperature coefficient of resistance, small low-temperature heat capacity and low thermal conductivity. The amount of the heat supplied to the addenda and sample was given by

$$\Delta Q = I_H V_H \Delta t \qquad (3.1)$$

where I_H is the current through the heater, V_H is the voltage drop across the heater and Δt is the time interval of the heat pulse. The current I_H was determined by the voltage drop across a 1 kΩ standard resistor. This voltage and V_H were measured by a 7500 Data Precision voltmeter. The Δt was recorded by a Monsanto 8510 50 MHz counter/timer.

The third part of the system was the GRT circuit. The GRT resistance was measured by the standard dc four-probe method. The GRT is chosen for this low temperature heat capacity work because of its independence on thermal history, small heat capacity and good temperature sensitivity. More details can be found in Yeh's thesis [27].

The heat capacity of the sample was found in the following way. A certain amount of the heat, ΔQ_{add} or ΔQ, was supplied to the addenda (consists of sample holder, heater and GRT) or addenda plus sample, respectively, to raise their temperature by ΔT. The heat capacity of the addenda, C_{add}, or sample, C, was found from the relationships

$$C_{add} = \frac{\Delta Q_{add}}{\Delta T} \tag{3.2}$$

or

$$C = \frac{\frac{\Delta Q}{\Delta T} - C_{add}(calc)}{X} \tag{3.3}$$

respectively, where $C_{add}(calc)$ was the calculated heat capacity of the addenda and X is the number of gram-atoms of the sample. The $C_{add}(calc)$ term could be determined separately [27].

IV. RESULTS AND DISCUSSION

A. Electrical Resistivity

The sample was cut into three ~0.5 in. long rectangular rod shapes by a diamond saw. These three vanadium specimens were indicated by A, B, and C for three different zones. In Figures 6 and 7, the resistivity as a function of temperature divided by the resistivity at room temperature is plotted for vanadium over the temperature range 4 to 300 K, which shows that the superconducting transition temperature is 5.41 K.

Van der Pauw [24] showed that the resistivity of a flat sample of thickness D with an arbitrarily-shaped perimeter could be calculated by solving the equation

$$\exp\left(-\frac{\pi R_{ab,cd} D}{\rho}\right) + \exp\left(-\frac{\pi R_{bc,da} D}{\rho}\right) = 1 \qquad (4.1)$$

for ρ, given the resistances $R_{ab,cd}$ and $R_{bc,da}$. Wires are attached at four points around the circumference of the sample and the contacts are cyclically designated a, b, c, and d. Resistance $R_{ab,cd}$ is defined as the potential difference $V_d - V_c$ between contacts d and c per unit current through contacts a and b; resistance $R_{bc,da}$ is defined similarly. Eq. (4.1) is valid if (i) the contacts are placed in successive positions along the circumference of the sample, (ii) the contacts are sufficiently small (relative to the size of the sample), (iii) the sample is uniform in thickness, and (iv) the sample contains

Figure 6. $\rho(T)/\rho(300\ K)$ versus T plot from 10 to 300 K for vanadium

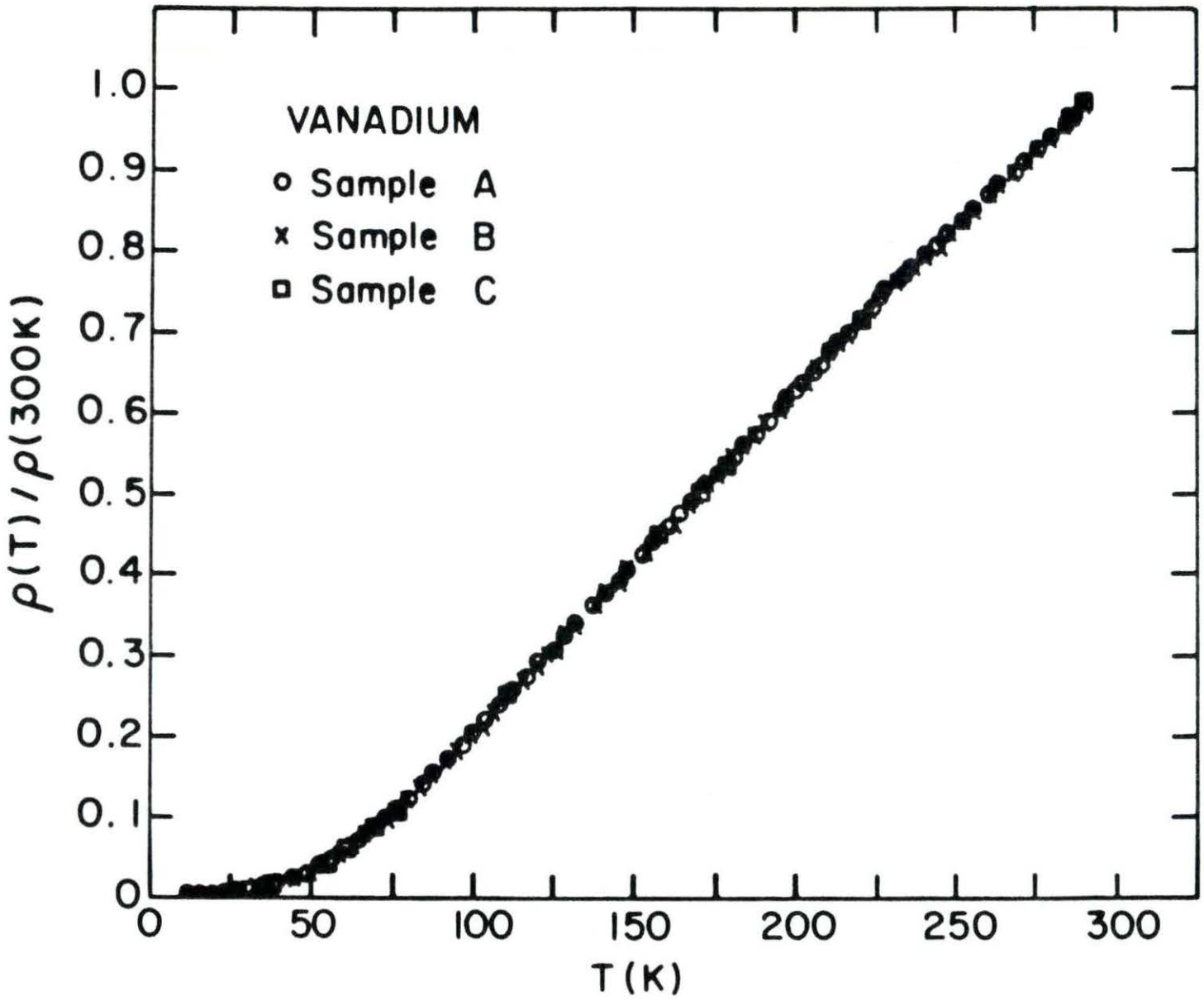
VANADIUM
o Sample A
x Sample B
□ Sample C
ρ(T)/ρ(300K)
T(K)
0
0.1
0.2
0.3
0.4
0.5
0.6
0.7
0.8
0.9
1.0
0
50
100
150
200
250
300

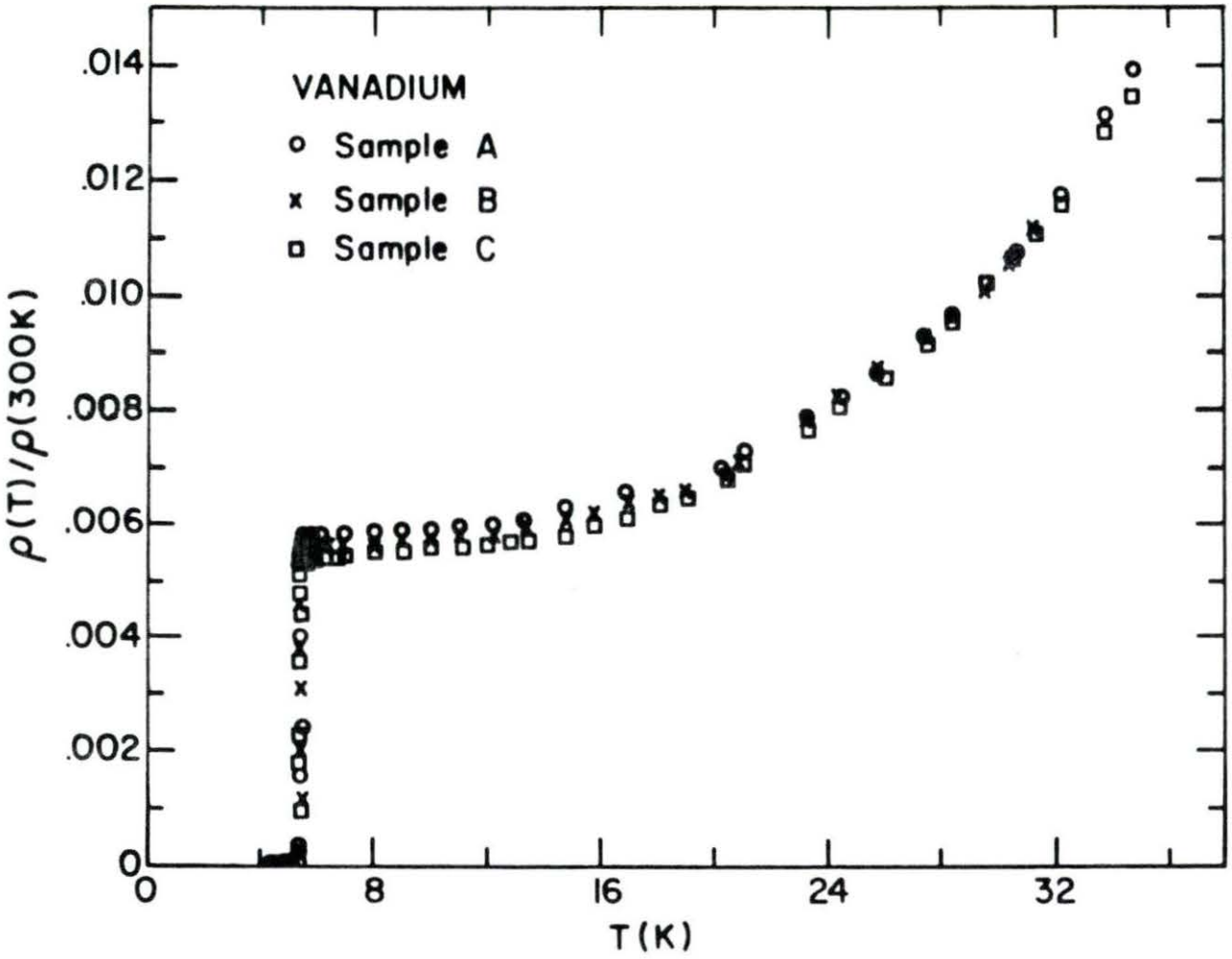

Figure 7. ρ(T)/ρ(300 K) versus T plot from 4 to 36 K for vanadium

no isolated holes. All these requirements were met by the samples used in this study. Because vanadium has a bcc structure, Eq. (4.1) can be changed as

$$2 \exp\left(-\frac{\pi R_{ab,cd} D}{\rho}\right) = 1 \ . \qquad (4.2)$$

Table 1 gives the resistivities at room (300 K) and liquid helium (~4.2 K) temperatures and the ratio $\Gamma_{4.2} = \rho(300\ K)/\rho(4.2\ K)$ for three different pieces cut from the A, B, C zones of the sample.

Table 1. Electrical resistivity values at 300 K and 4.2 K and the resistance ratio, $\Gamma_{4.2}$, for vanadium

Zone	ρ(300 K) ($\mu\Omega$-cm)	ρ(4.2 K) ($\mu\Omega$-cm)	$\Gamma_{4.2}$ = ρ(300 K)/ρ(4.2 K)
A	19.93	0.114	175
B	20.0	0.108	185
C	20.0	0.105	190

B. Upper Critical Field

Figure 8 shows the magnetic susceptibility, χ, versus temperature from 1.5 K to room temperature. The absence of any peaks or minima in the χ over this temperature interval indicates that spin fluctuation contribution is small, compared to that found in normal spin fluctuators [14].

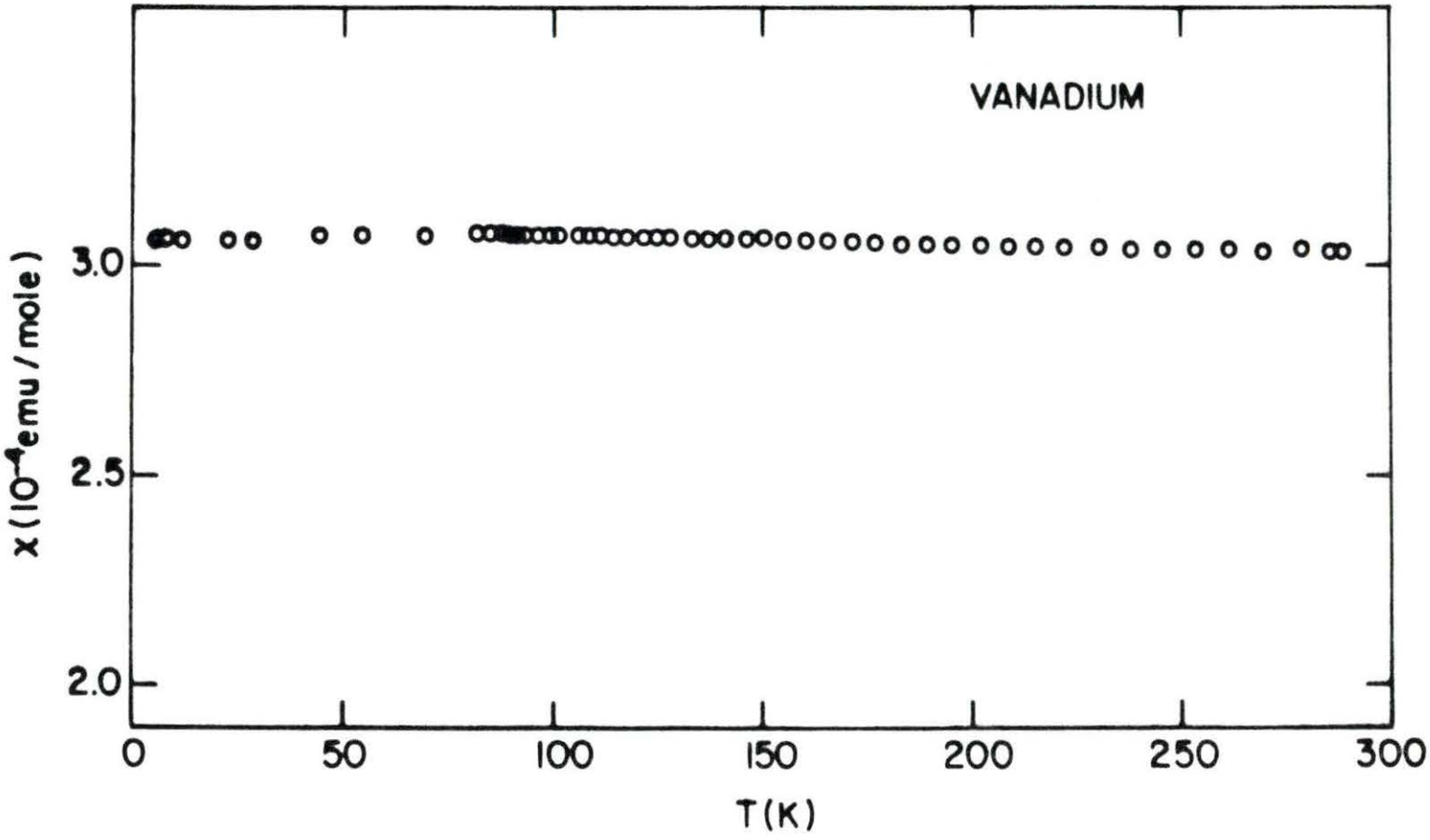

Figure 8. The magnetic susceptibility versus T for vanadium

The upper critical field measurements as a function of temperature were made resistively, as described earlier. The observed $H_{c2}(T)$ versus T and $H_{c2}(T)$ versus t^2 ($t = T/T_c$) are shown in Figures 9 and 10, respectively.

C. Heat Capacity

The heat capacity measurements were made between 1.3 and 20 K for the vanadium specimen at magnetic fields of 0, 1.25, 2.5, 5.39, 7.62 and 9.98 T. Figure 11 shows the C/T versus T^2 plots for vanadium over the temperature range from 1.5 to 10 K. The temperature at which superconducting begins, T_c^*, and the midpoint transition temperature, T_c, are summarized in Table 2. The zero field C/T versus T^2 plot for vanadium is shown in Figure 12.

The normal state portions of C/T versus T^2 curve were analyzed by using Eq. (2.9). Values of γ, β and θ_D were obtained by a least-squares fit of the data for $T > 5.5$ K at zero field and all the high field data for $T > 1.5$ K (see Table 2). The temperature range was selected in the linear region of the C/T versus T^2 plot. The Debye temperature, θ_D, was calculated from the Eq. (2.8). The temperature ranges over which the data were fitted are also listed in Table 2.

Figure 13 shows schematically the method used to determine the jump in the heat capacity (ΔC) at the superconducting transition temperature, T_c. The ΔC(obs) value for vanadium is given in Table 3. Table 3 also lists the value of $\Delta C/\gamma T_c$ which is slightly larger than the predicted BCS value of 1.43 (see Eq. (2.14)).

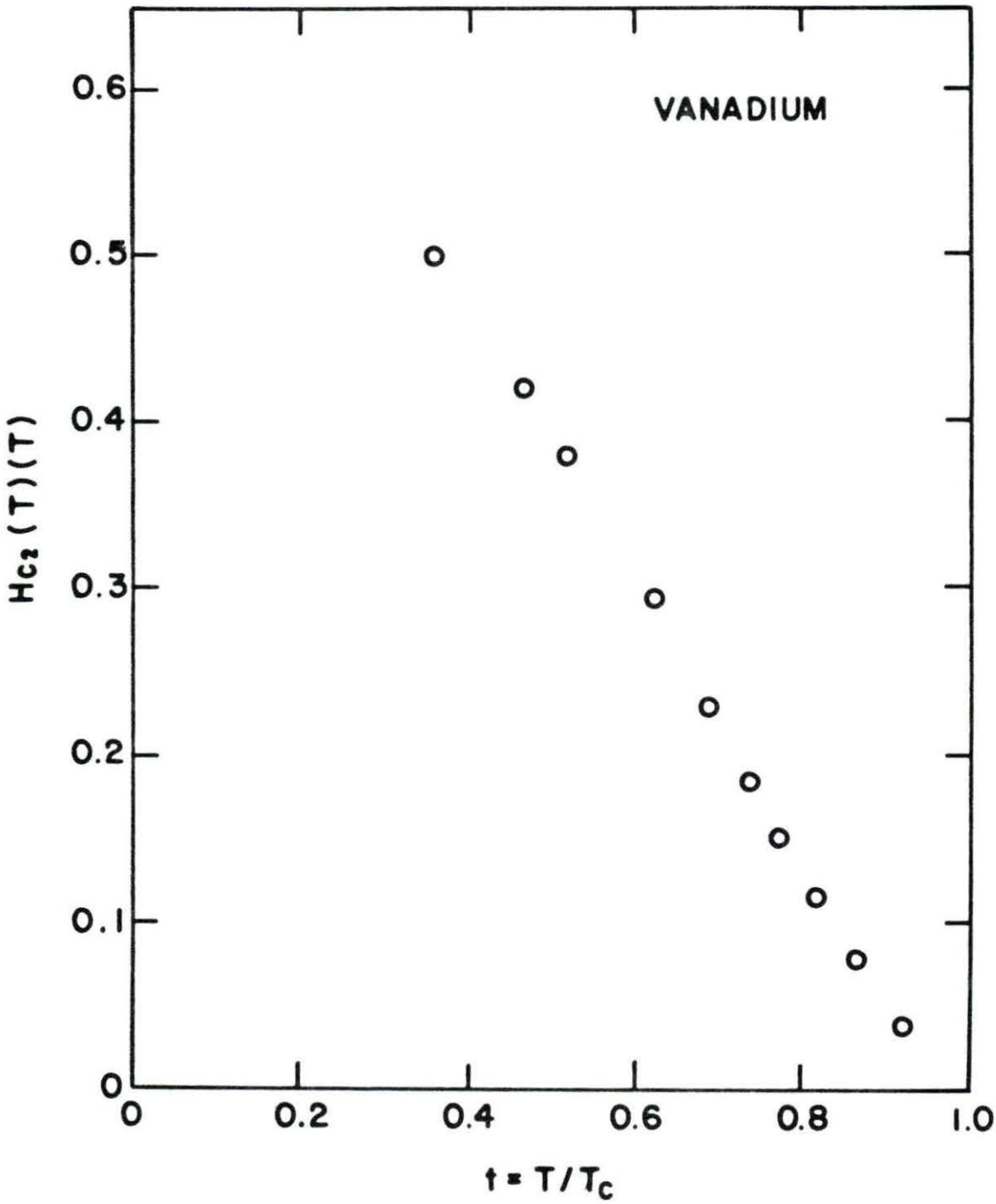

Figure 9. H_{c2} (T) vs. t for vanadium

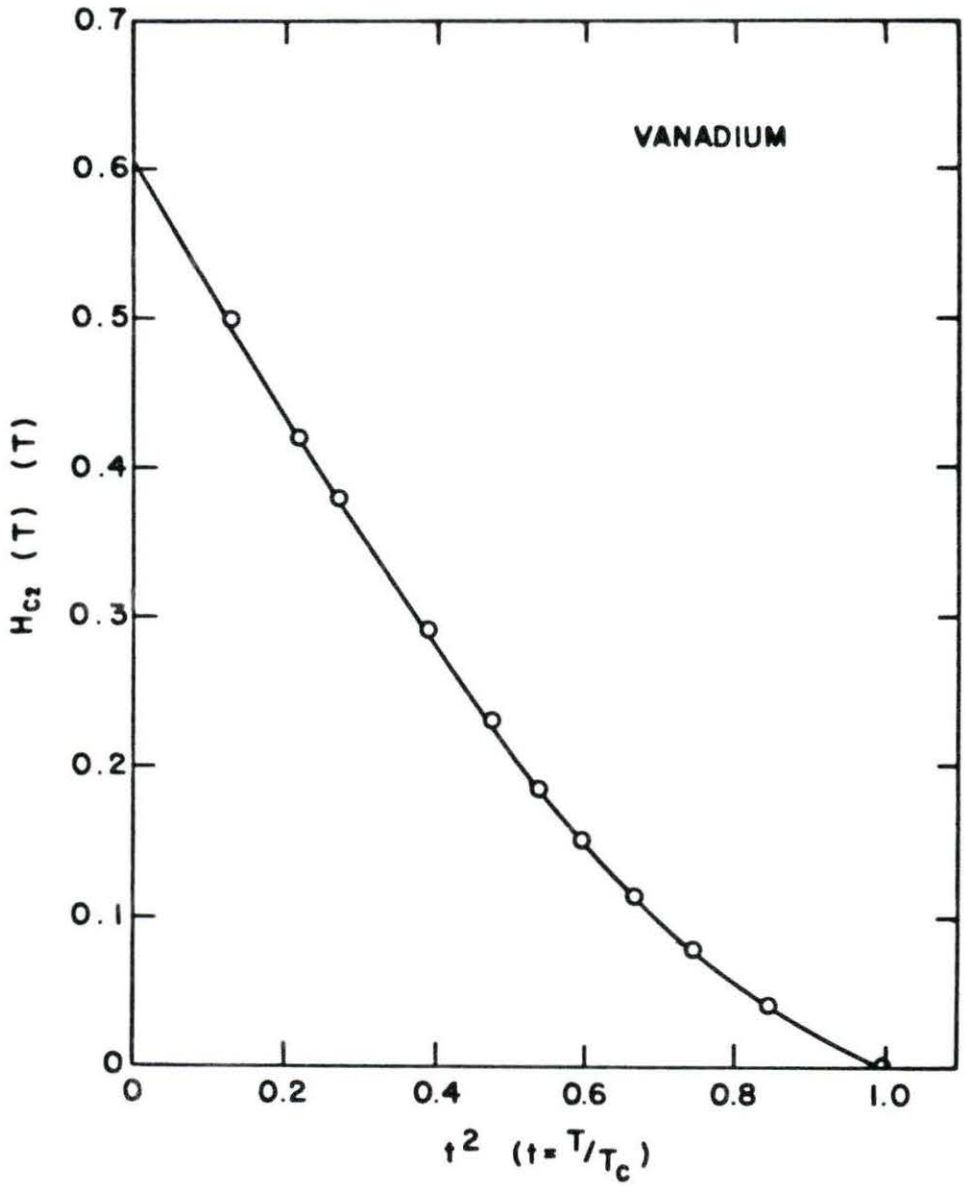

Figure 10. H_{c2} (T) vs. t^2 plot for vanadium

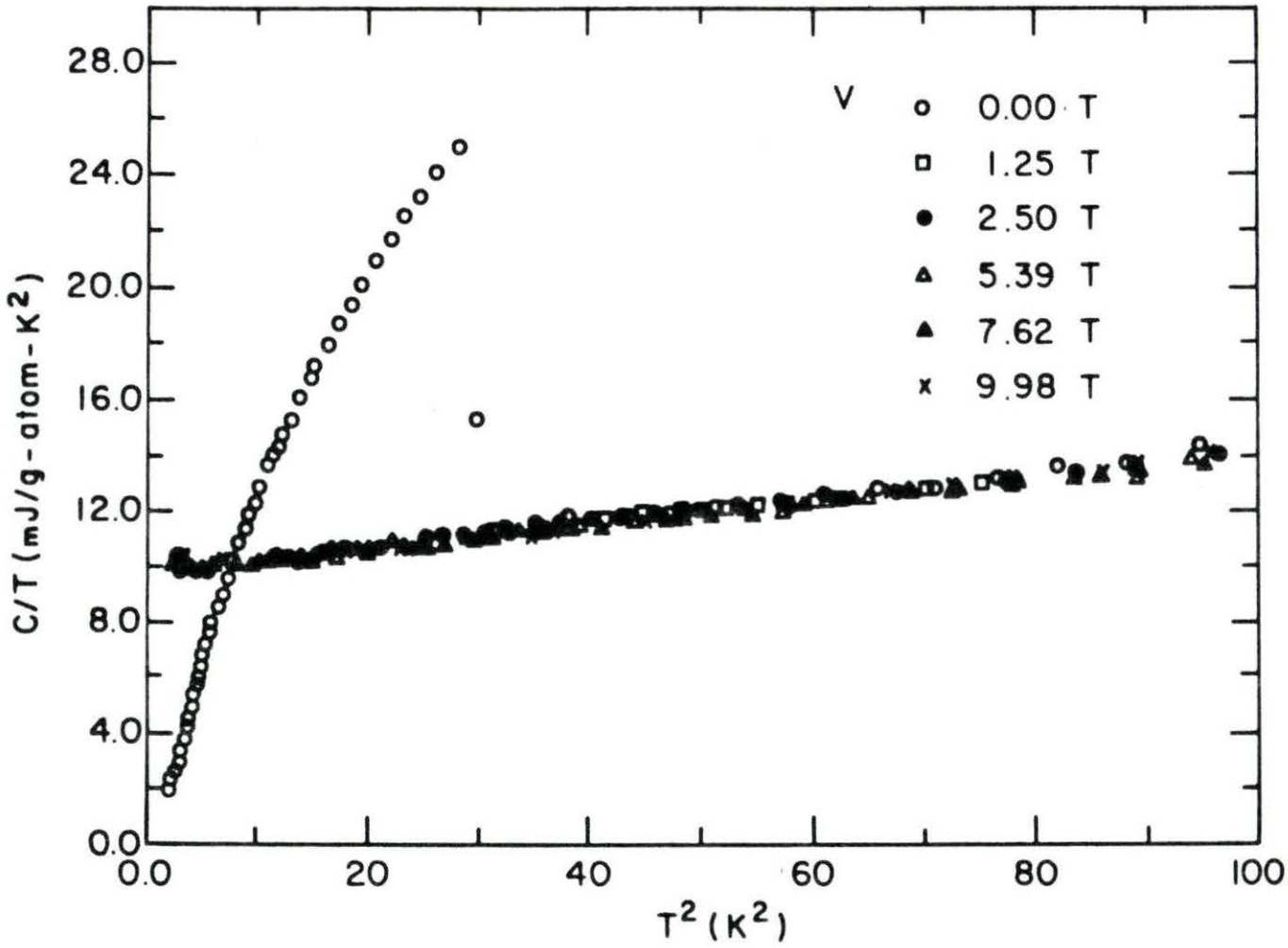

Figure 11. A plot of C/T versus T^2 from 1.5 to 10 K for vanadium

Table 2. The results of the heat capacity measurements of V: the values of the γ, β, θ_D and the temperature range for the least-squares fitting in different magnetic fields as well as T_c, T_c^* in zero magnetic field

H (T)	γ $[\frac{mJ}{g\text{-at-}K^2}]$	β $[\frac{mJ}{g\text{-at-}K^4}]$	θ_D (K)	Temp. range of fit (K)	T_c (K)	T_c^* (K)
0.00	10.0 $\pm$ 0.1	0.042 $\pm$ 0.002	360 $\pm$ 4	5.6 - 8.2	5.41	5.56
1.25	9.98 $\pm$ 0.02	0.0437 $\pm$ 0.0008	354 $\pm$ 2	2.6 - 7.0		
2.50	9.82 $\pm$ 0.01	0.0433 $\pm$ 0.0004	355 $\pm$ 1	1.6 - 9.8		
5.39	9.80 $\pm$ 0.01	0.0435 $\pm$ 0.0005	355 $\pm$ 1	1.5 - 7.0		
7.62	9.79 $\pm$ 0.02	0.0422 $\pm$ 0.0009	358 $\pm$ 2	1.5 - 6.9		
9.98	9.79 $\pm$ 0.02	0.0425 $\pm$ 0.0009	358 $\pm$ 2	1.7 - 7.0		
Whole data avg.	9.80 $\pm$ 0.08	0.0441 $\pm$ 0.0003	355 $\pm$ 1	1.5 - 9.8		

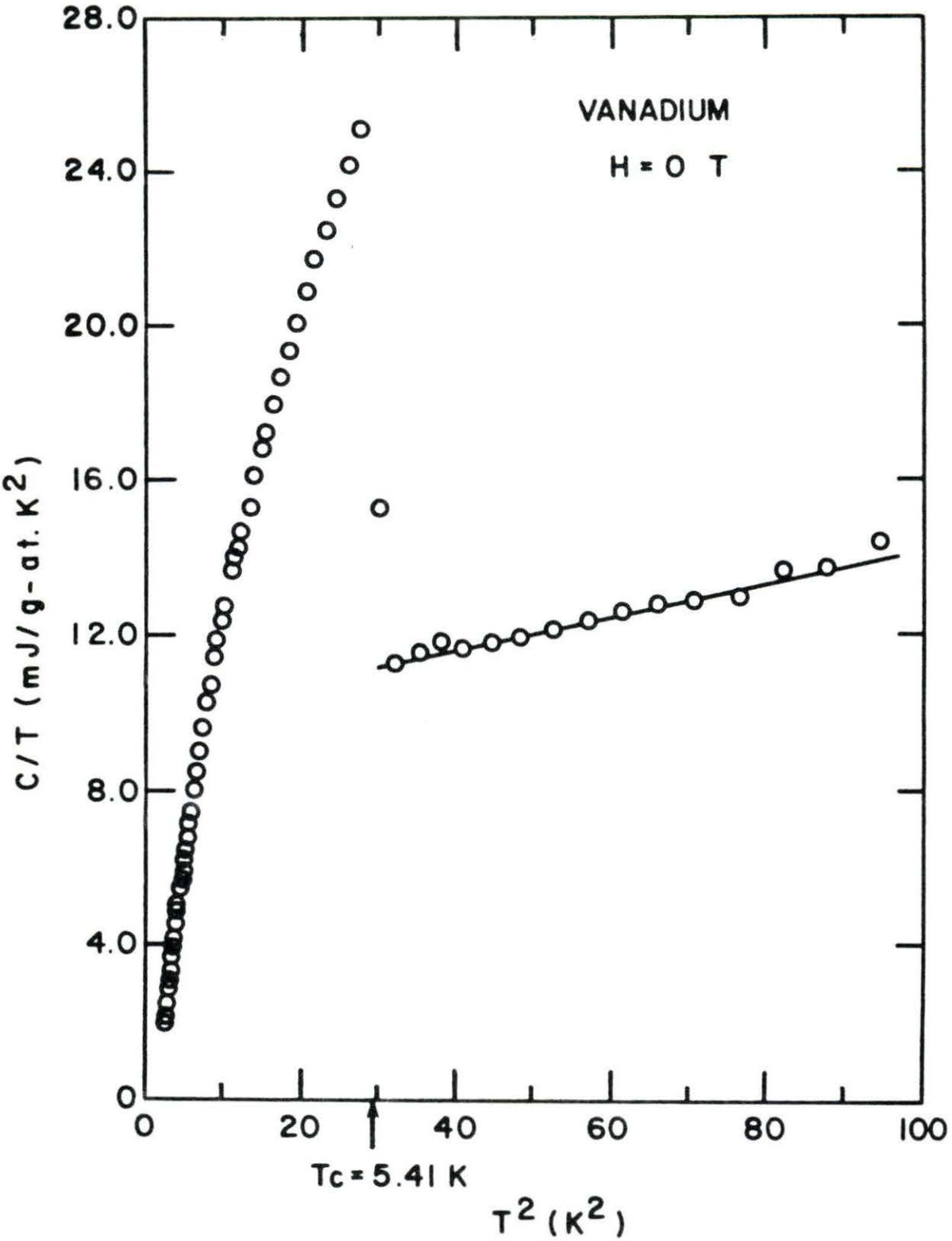

Figure 12. A plot of C/T versus T^2 for vanadium at zero field

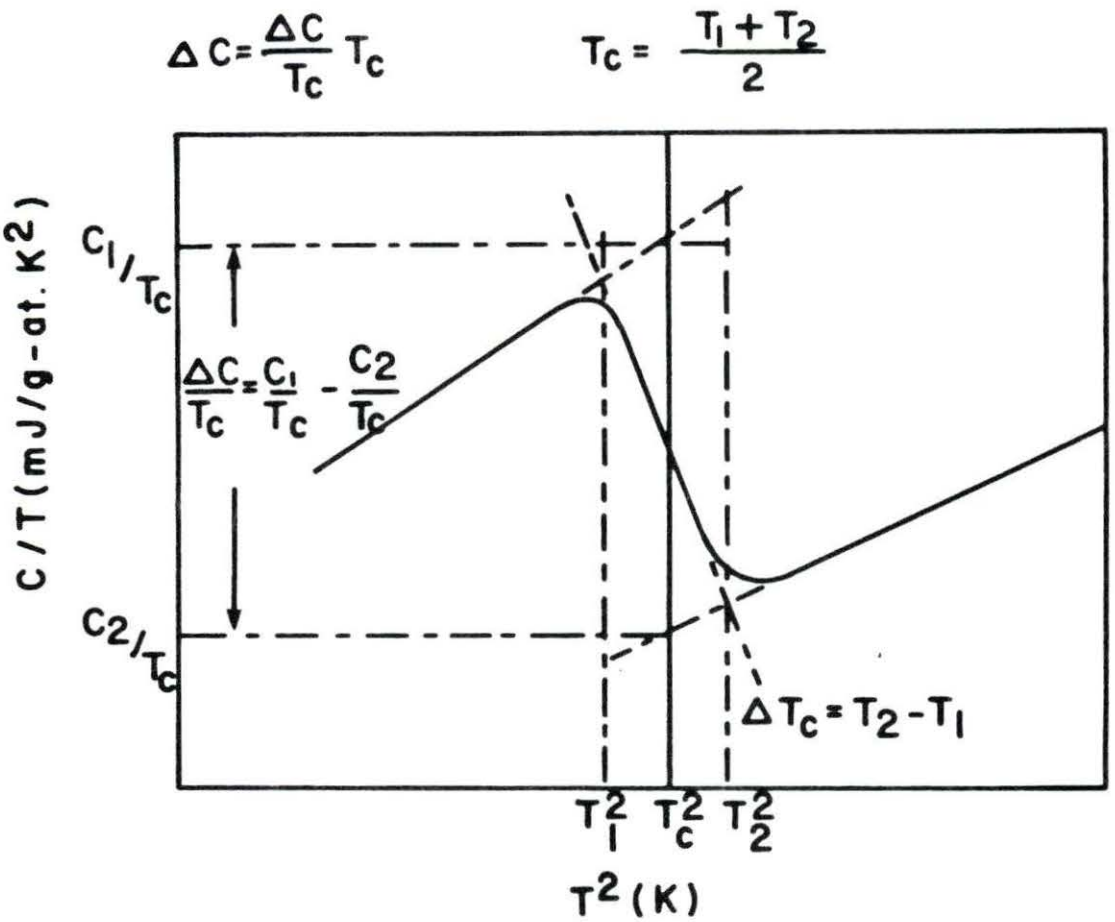

Figure 13. Method shown schematically to determine the jump in the heat capacity at the superconducting temperature, ΔC, the superconducting temperature, T_c, and the width of the transition, ΔT_c

Table 3. Molar volume V; maximum superconducting temperature, T_c^*; entropy values at T_c^* in the normal and superconducting states; the percentage difference between S_n and S_s, ΔS; thermodynamic critical field at 0 K, $H_c(0)$; jump in the heat capacity at T_c, ΔC; measured value of the reduced jump in the heat capacity at T_c, $\Delta C/\gamma T_c$; reduced energy gap, $2\Delta(0)/kT_c$; the parameters a and b from the reduced superconducting state electronic heat capacity expression Eq. (2.11); the electron-phonon coupling parameter, λ; and the experimental electronic density of state at the Fermi surface, $N(0)_{exp}$ for vanadium

V $[\frac{cm^3}{g\text{-}at}]$	T_c^* (K)	S_n $[\frac{mJ}{g\text{-}at\ K}]$	S_s $[\frac{mJ}{g\text{-}at\ K}]$	ΔS (%)	$H_c(0)$ (T)	$\Delta C(calc)$ $[\frac{mJ}{g\text{-}at\ K}]$	$\Delta C(obs)$ $[\frac{mJ}{g\text{-}at\ K}]$
8.34	5.65	57.8	57.5	0.5	0.143	93.2	79.4

(ΔC) (%)	$\frac{\Delta C(obs)}{\gamma T_c}$	$\frac{2\Delta(0)}{k T_c}$ (calc)	$\frac{2\Delta(0)}{k T_c}$ (obs)	a	b	λ_{ep}	$N(0)_{exp}$ $[\frac{state}{eV/at}]$
14.8	1.46	3.51	3.51	8.48	1.435	0.6	4.16

As described previously in Chapter II, the entropy, S, at T can be obtained from the integration of C/T with T as expressed in Eq. (2.15). The normal state data above T_c^* were taken from the data in 9.98 T and below T_c^* (in 0 T), were taken from the Eq. (2.9). At T_c^*, S_n should equal S_s. The entropy versus T plot is given in Figure 14. The values of S_n and S_s at T_c^* and the percentage difference between them for vanadium are listed in Table 3. The good agreement of the resultant entropies (within 0.5%) indicates that γ, β and θ_D values obtained from this method are valid.

The electronic heat capacity in the superconducting state, C_{es}, can be determined from Eq. (2.10). The semilog plots of the reduced superconducting electronic heat capacity, C_{es}/T_c, versus T_c/T (from 1 to 4.5) are shown in Figure 15. The experimental values agree well with the BCS theory prediction for a weak-coupling superconductor. The value of the energy gap, $2\Delta(0)$, can be obtained based on the assumptions that [28]: (i) $\Delta(T)$ is independent of the energy and isotropic, and (ii) $\Delta(T)/\Delta(0)$ is identical to that given by BCS theory. The value of the reduced energy gap, $2\Delta(0)/k\,T_c$ (obs), can be determined from the slope of the curve in Figure 15 by the relation

$$\frac{2\,\Delta(T)}{k\,T_c} = \frac{3.52b}{1.44}$$

$$= 2.44b \qquad (4.3)$$

where b is the negative of the slope value and was defined in Eq. (2.11),

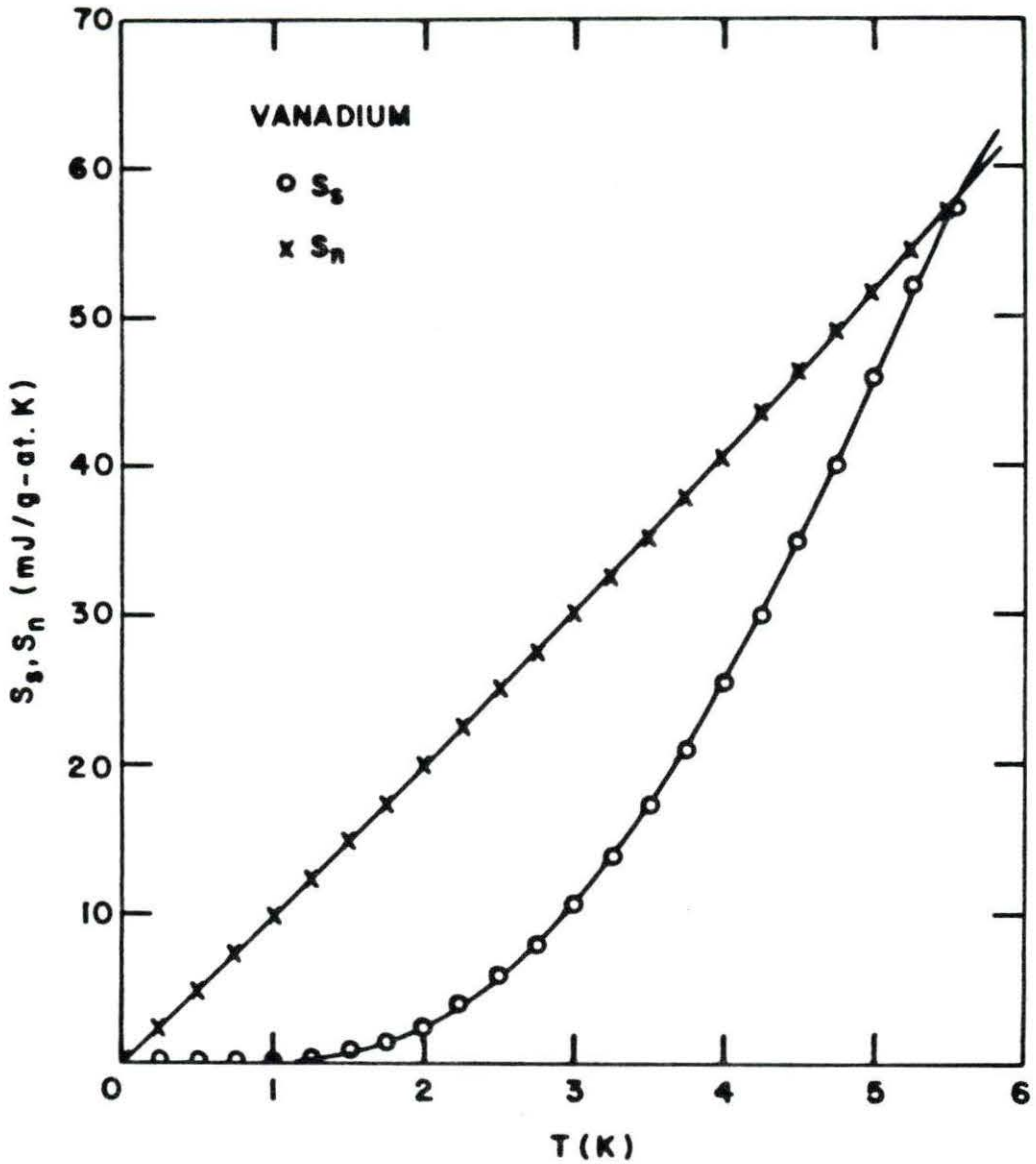

Figure 14. A plot of entropy versus T(K) for vanadium

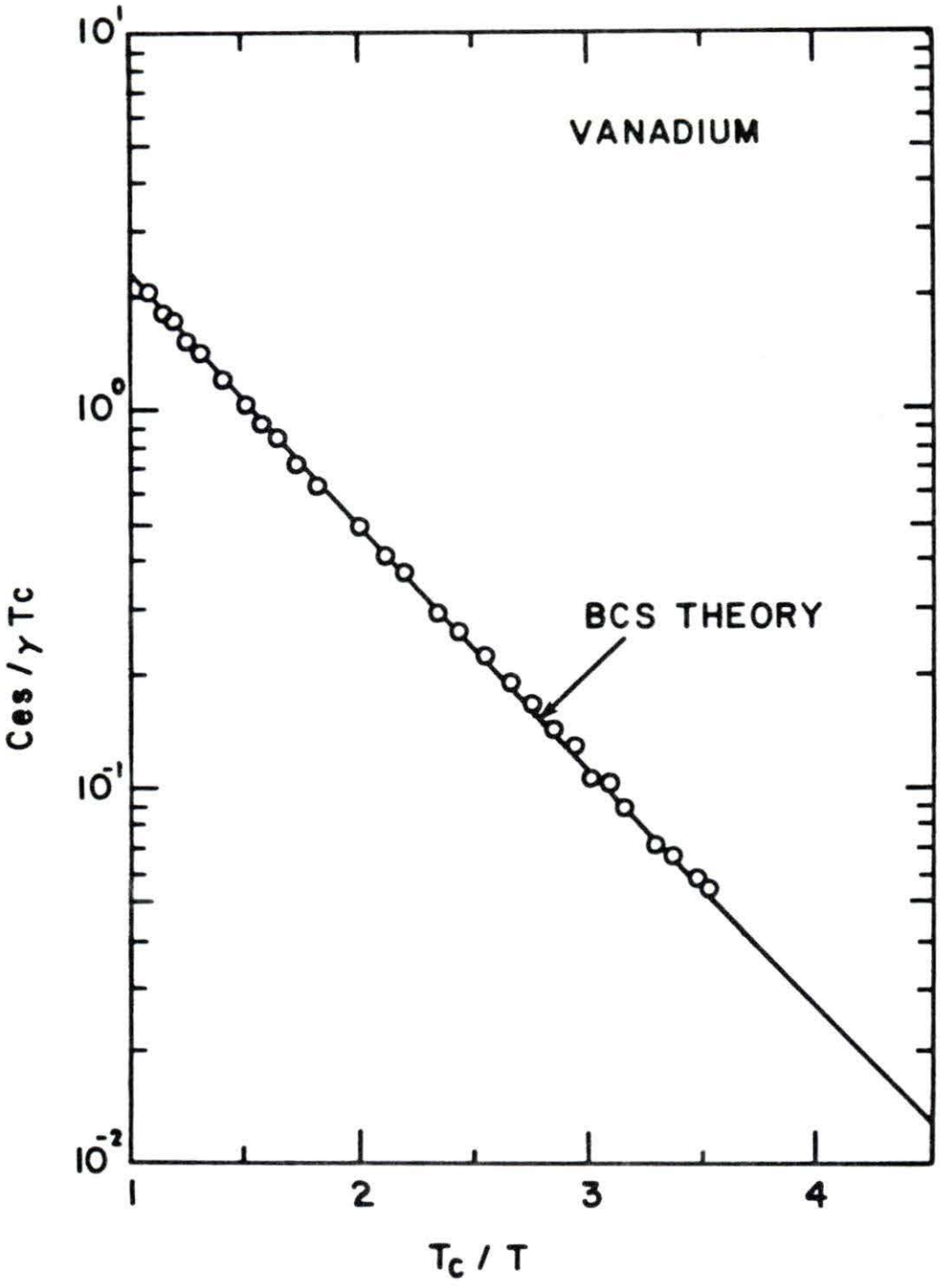

Figure 15. Reduced superconducting electronic heat capacity of vanadium

3.52 is the value from the BCS theory and 1.44 is taken from Eq. (2.12). The ranges of T_c/T for the slope determination, the value of the reduced energy gap obtained from Eq. (4.3), a and b (defined in Eq. (2.11)) are listed in Table 3. It is seen that the observed values of the reduced energy gap are very close to the BCS prediction of 3.53.

The Gibbs free energy can be obtained from the Eq. (2.16). Its values in the normal and superconducting states are plotted in Figure 16 in which the U + (PV) terms are neglected since they remain the same in both states. From Eq. (2.19b), $H_c(T)$ can be calculated from the difference between $G_n(T)$ and $G_s(T)$. $V = 8.34\ cm^3\ mole^{-1}$ is the molar volume for vanadium [29]. The $H_c(T)$ versus T plot is shown in Figure 17, and the $H_c(0)$ value is listed in Table 3.

According to Eq. (2.20), the relationship between the $H_c(T)$ and t^2 ($t = T/T_c$) is linear, and this seems to be true for vanadium, as shown in Figure 18. The deviation function, D(t), is defined as

$$D(t) = \frac{H_c(t)}{H_c(0) - (1 - t^2)} \quad . \tag{4.4}$$

The D(t) versus t^2 plot is shown in Figure 19, comparing with the BCS prediction. The departure from the BCS theory curve at $t^2 > 0.2$ suggests that vanadium is weak-coupling type-II superconductor.

The jump in the heat capacity at T_c in zero field, ΔC, can be calculated by using the Rutgers' relation [16, 30]

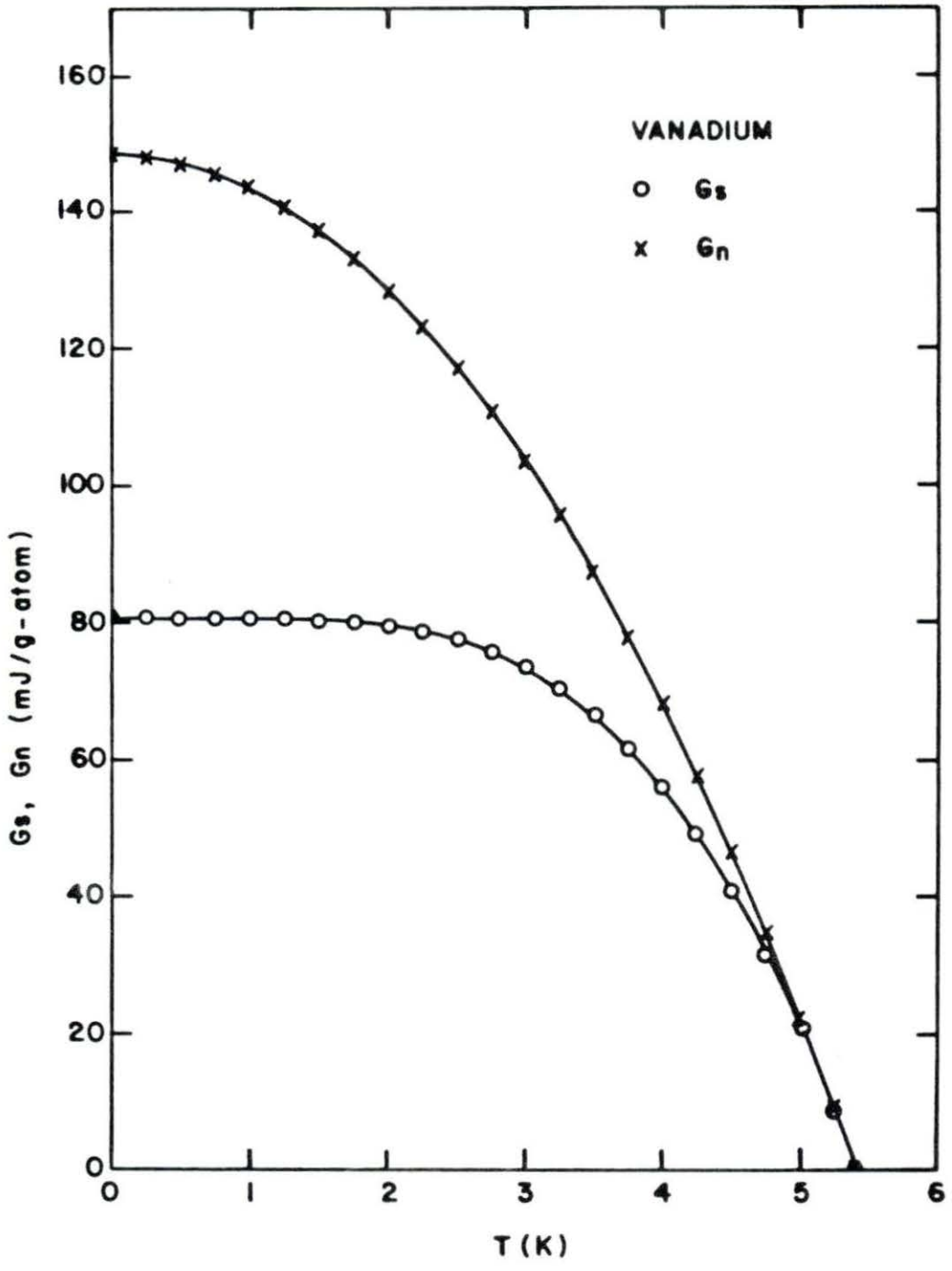

Figure 16. The Gibbs free energy versus T for vanadium

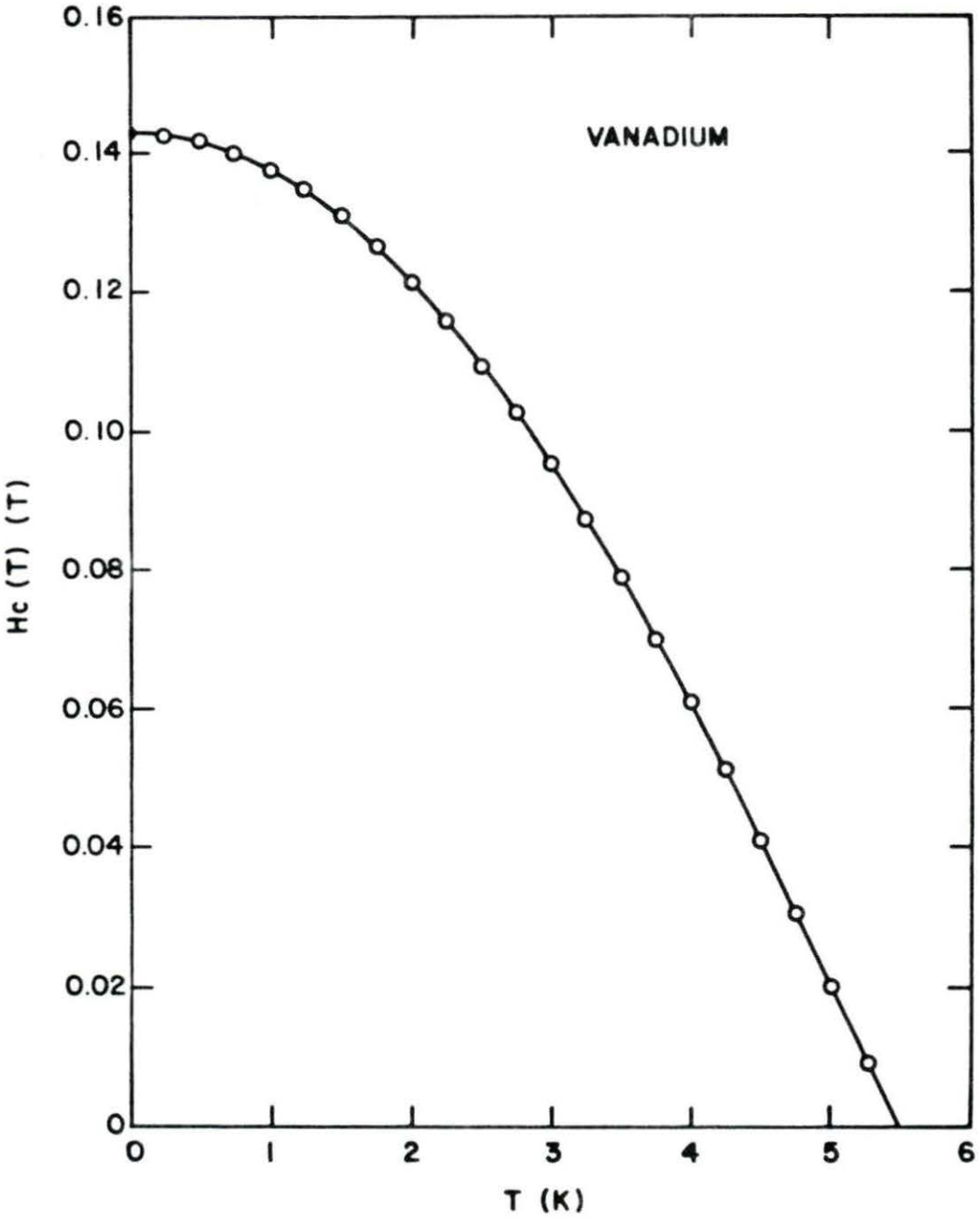

Figure 17. $H_c(T)$ versus T plot for vanadium

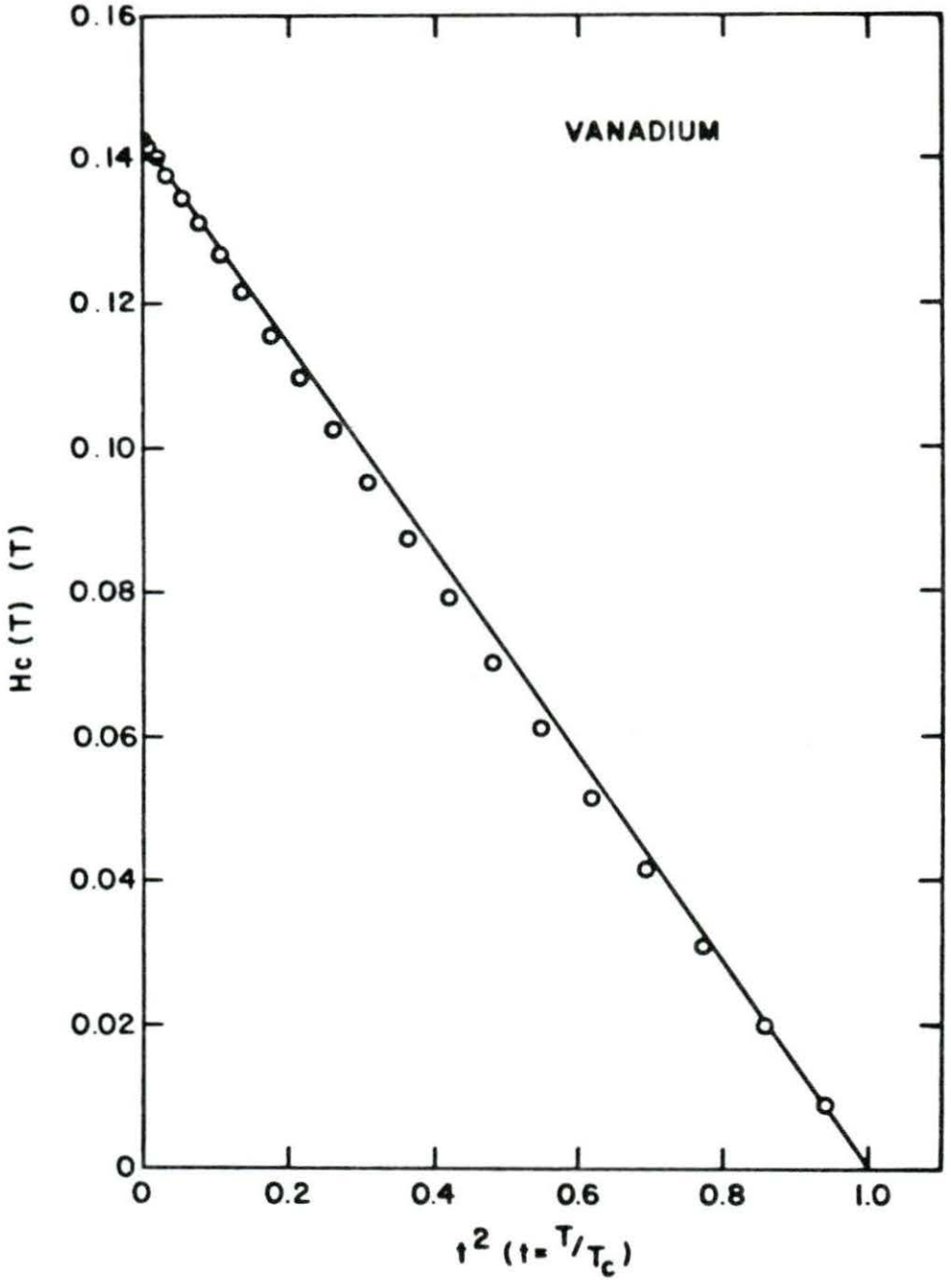

Figure 18. $H_c(T)$ versus t^2 for vanadium

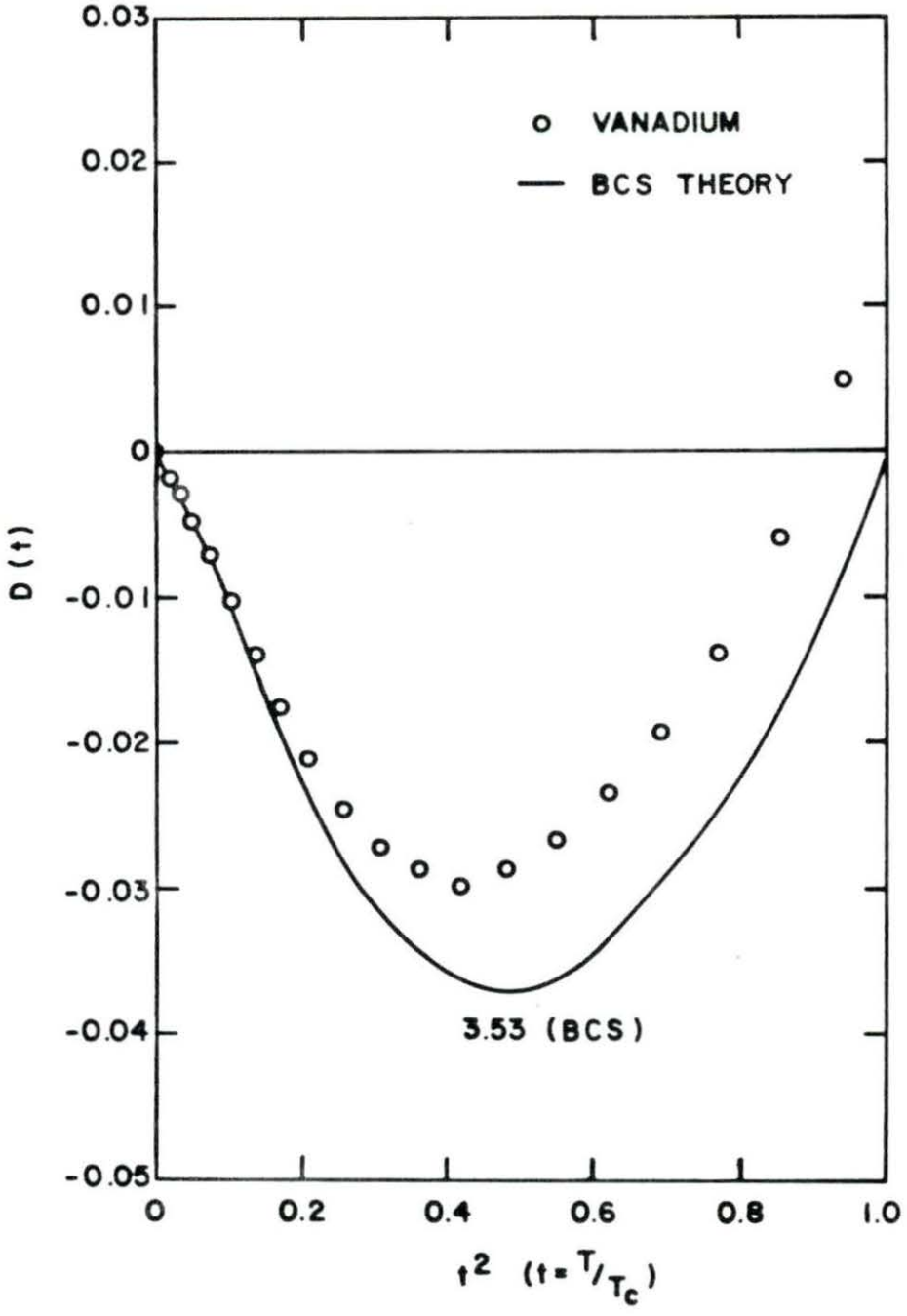

Figure 19. The D(t) versus t^2 plot for vanadium

$$\Delta C(\text{calc}) = \frac{V\, T_c}{4} \left[\frac{d\, H_c(T)}{dT}\right]^2_{T = T_c} \qquad (4.5)$$

Eq. (2.20) has been used to calculate the slope of the $H_c(T)$ versus T at T_c. The $\Delta C(\text{calc})$ value is compared to the $\Delta C(\text{obs})$ found experimentally and is given in Table 3. It was seen that there was a large difference between the two ΔC values. The slopes of the $H_c(T)$ versus T at T_c in Eq. (4.5) probably are the main reason which made the difference. The $\Delta C(\text{obs})$ value is probably more reliable than $\Delta C(\text{calc})$.

According to Goodman [31], the values of the reduced energy gap at T = 0 can be obtained from the relation

$$\frac{2\Delta(0)}{k\, T_c}(\text{calc}) = \frac{4\pi}{\sqrt{3}} \left[\frac{H_c(0)^2\, V}{8\pi\, \gamma\, T_c^2}\right]^{1/2} . \qquad (4.6)$$

Using the values of $H_c(0)$, V, γ and T_c given in Tables 2 and 3, the energy gap for vanadium was calculated. Compared to the values obtained from Eq. (4.3) and listed in Table 3, they were found to be in good agreement and are very close to the BCS prediction of 3.53.

McMillan [32] explained theoretically that the transition temperature is given by

$$T_c = \frac{\theta_D}{1.45} \exp\left[-\frac{1.04\,(1 + \lambda_{ep})}{\lambda_{ep} - \mu^*(1 + 0.6\,\lambda_{ep})}\right] \qquad (4.7)$$

where λ_{ep} is the electron-phonon coupling parameter, and μ^* is the repulsive electron-electron interaction parameter (taking $\mu^* = 0.12$ which is lowest value in [33] and highest value in [34]). Moreover, the electronic specific heat parameter, γ, is enhanced by the factor $(1 + \lambda)$ from the electron-phonon interaction. If λ_{ep} and γ are known, the electronic density of states at Fermi surface at 0 K, N(0), can be calculated by using Eq. (2.6). The values of λ_{ep} and N(0) are listed in Table 3.

The upper critical field, $H_{c2}(T)$, is related to the critical thermodynamic field, $H_c(T)$, by the parameter κ_1 defined in Eq. (2.21). The $\kappa_1(T)$ versus t^2 is plotted in Figure 20. The solid line in Figure 20 is the result of least-square fitting. $\kappa_1(1) = 0.85$ as extrapolating to $t^2 = 1$.

The $\kappa_2(T)$ values were estimated by Eqs. (2.22) and (2.24). At T equal to T_c, $\kappa_2(1) = 1.12$. According to Eq. (2.23), the κ value can be determined from κ_1 $(t = 1)$ or κ_2 $(t = 1)$. Maki and Tsuzuki [35] pointed out that $\kappa_2(t) \geq \kappa_1(t)$ for all temperatures. This is in agreement with the present results on vanadium. Therefore, the Ginzburg-Landau parameter, κ, is taken as $\kappa_1(1) = 0.85$, which is always the minimum value of $\kappa_1(t)$. For this sample of vanadium, the ratio $\Gamma_{4.2}$ is 190 and ρ_r is 0.105×10^{-6} Ω cm, as shown in Table 1. The result of $\kappa_\ell = 0.086$ is then obtained from Eq. (2.26). The experimental value of $\kappa \equiv \kappa_1(1)$ is 0.85, so that κ_0 equals 0.764 from Eq. (2.25). Since $\kappa_0 > 1/\sqrt{2}$, this result then shows that vanadium is an intrinsic type-II superconductor.

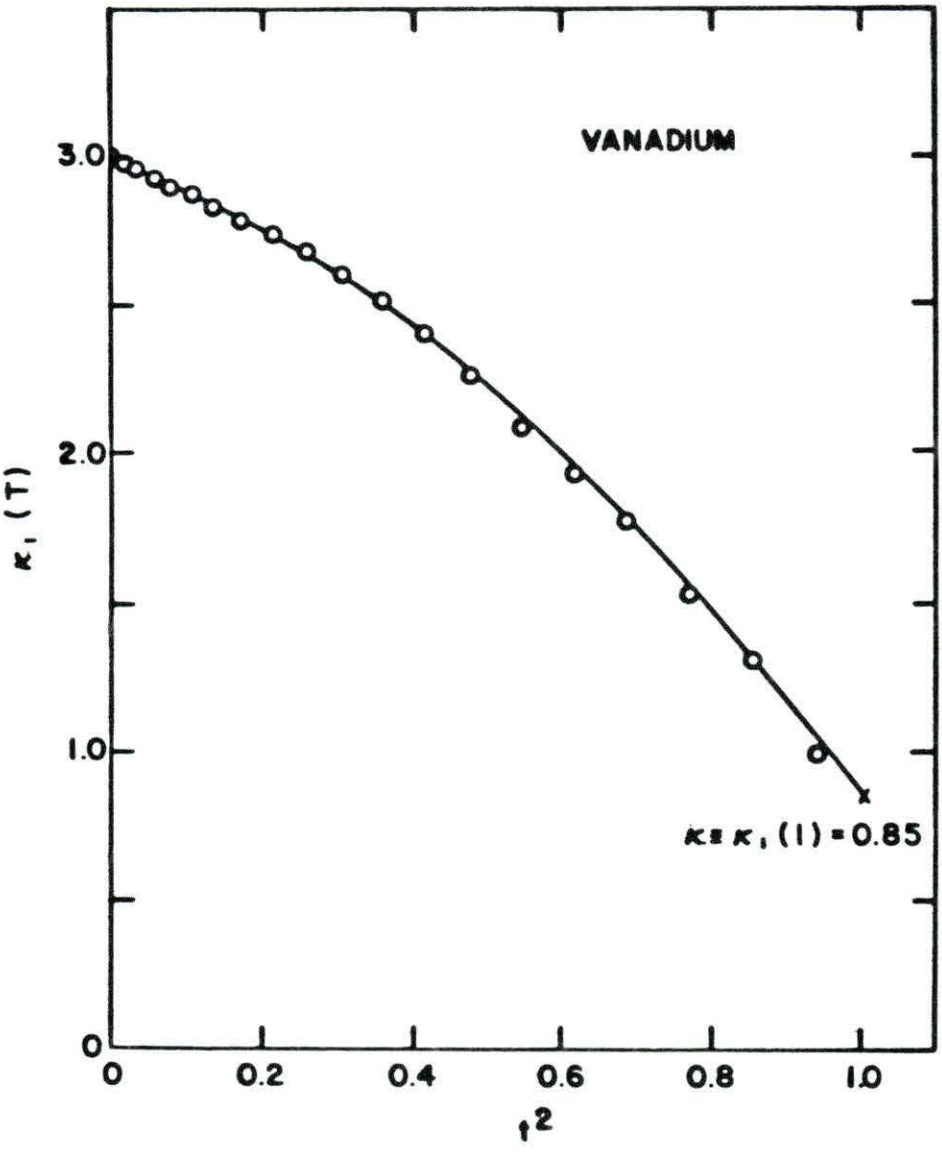

Figure 20. The generalized Ginzburg-Landau parameter $\kappa_1(T)$ versus t^2 where $t = T/T_c$ for vanadium

The specific heat can be used to calculate several other superconducting and normal-state parameters as mentioned in Chapter II. The values of the intrinsic coherence length, ξ_0; the London parameter depth, $\lambda_L(0)$; the area of the Fermi surface in k-space excluding zone boundaries, S; the electron mean free path, ℓ; and the average Fermi velocity, V_F, can be calculated from Eqs. (2.28) to (2.32), respectively.

Table 4 summarizes several electronic properties of pure vanadium determined from this investigation just previously defined and compared with the results of Radebaugh and Keesom [10]. From $\ell/\xi_0 = 6.66$, this sample, then, is definitely a "clean" superconductor.

For vanadium, using the specific-heat measurements $\gamma = 9.8$ mJ/mole K^2 and the density of state from band-structure calculations, $N(0)_{BS} = 0.90$ states/spin eV·atom, and using the relation

$$\frac{m^*}{m} = \frac{3\gamma}{2\pi^2 k^2 N(0)} \quad , \tag{4.8}$$

gives

$$\frac{m^*}{m} = \frac{N(0)_{exp}}{N(0)_{BS}} = \frac{\gamma_{exp}}{\gamma_{BS}} = 1 + \lambda \tag{4.9}$$

where

$$\frac{N(0)_{exp}}{N(0)_{BS}} = \frac{2.079}{0.9} = 2.31 \quad . \tag{4.10}$$

Table 4. Summary of several electronic parameters of pure vanadium comparing with Radebaugh and Keesom's results [10]

Parameter	This work	Radebaugh & Keesom [10]
γ(mJ-mole^{-1}K^{-2})	9.8	9.82
γ(erg-cm^{-3}K^{-2})	1.175	1.179
T_c (K)	5.41 $\pm$ 0.01	5.414 $\pm$ 0.010
κ_0	0.764	0.848
$\kappa \equiv \kappa_1$ (T_c)	0.85	0.979
S/S_F	0.752	0.714
S (cm^{-2})	4.58×10^{17}	4.35×10^{17}
$\lambda_L(0)$ (Å)	377	398
ξ_0 (Å)	475.5	450
ℓ (Å)	3183.0	2450
ℓ/ξ_0	6.69	5.44
V_F (cm-sec^{-1})	0.185×10^8	0.177×10^8
τ_{tr} (sec)	1.7×10^{-12}	1.4×10^{-12}

Substituting Eq. (4.10) into Eqs. (4.9) and (2.44) yields

$$\lambda_{spin} = 1.31 - 0.6 = 0.71 \quad . \qquad (4.11)$$

The electron mass enhancement m^*/m value (2.31) from this study is close to the theoretical value $(m^*/m)_{T_c} = 2.38$ calculated based on the Eliashberg equations [12].

Table 5 lists the experimental data from Radebaugh and Keesom [10] and the theoretical data from Rietschel [13], along with the results obtained in this study. The λ_{spin} value from this work is about twice of the theoretical value in the second and fourth rows of Table 5. But, comparing to the λ_{spin} values in Ref. [14], the λ_{spin} of vanadium is quite small, and this is probably why no effect of the applied magnetic field on γ was observed as had been found in other spin fluctuation materials [14]. These results are also consistent with the flat, temperature independent magnetic susceptibility of vanadium in that there is no rapid rise in χ as T goes to 0 K (magnetic susceptibility tail), nor any high temperature maximum in the χ versus T plot found in most other spin fluctuators [14].

Table 5. Experimental [Ref. 10 and this work] and theoretical values of thermodynamic quantities in vanadium; model A: full account of spin fluctuation; model B: spin fluctuation neglected; and model C: best fit to the experimental results of Radebaugh & Keesom [10] [13]

	γ $[\frac{mJ}{mole\ K^2}]$	$H_c(0)$ [gauss]	ΔC $[\frac{mJ}{mole\ K}]$	λ_{ep}	λ_{spin}	$\Delta C/\gamma\ T_c$
Radebaugh & Keesom's experiment [10]	9.82	1421	78.6			1.48
Model A	10.6	1497	88.5	1.05	0.35	1.55
Model B	7.2	1231	57.5	0.63	0	1.48
Model C	9.7	1433	83.0	0.92	0.27	1.58
This work	9.8	1429	79.4	0.6	0.71	1.46

V. CONCLUSIONS

This work has shown that specific heat measurement is a powerful tool for determining the behavior of type-II superconductors with small lattice specific heats. The specific heat above H_c, unlike magnetization, is shown to be independent of sample history, and a complete thermodynamic description of the mixed state is derived. The thermodynamic critical field, H_c, is defined unambiguously from specific heat data in the superconducting and normal states alone.

It has been shown that vanadium, like niobium, is an intrinsic type-II superconductor since $\kappa_0 = 0.764 > 1/\sqrt{2}$. The mixed state properties of vanadium are much like that of niobium ($\kappa_0 = 0.76$). It has been suggested [36] that the discrepancy between GLAG (Ginzburg and Landau, Abrikosov and Gor'kov) theory and experiment may be a result of the failure to include nonlocal electrodynamic effects in the theory.

In this work, the investigations of the magnetic field dependence of the heat capacity and the temperature dependence of the magnetic susceptibility were used to see if there is any evidence for spin fluctuations which were thought to be present in vanadium. The results show that the spin fluctuation contribution is small.

VI. REFERENCES

1. H. K. Onnes, Comm. Kamerlingh Onnes Lab. Univ. Leiden, Suppl. 34B, 55 (1913).

2. H. K. Onnes, Comm. Phys. Lab. Univ. Leiden 119b, 1 (1911).

3. H. K. Onnes, Comm. Phys. Lab. Univ. Leiden 139f, 8 (1914).

4. W. Meissner and R. Ochsenfeld, Naturwissen 21, 787 (1933).

5. C. J. Gorter and H. B. G. Casimir, Physica 1, 306 (1934).

6. F. London and H. London, Proc. Roy. Soc. A149, 71 (1935); Physica 2, 341 (1935).

7. A. B. Pippard, Proc. Roy. Soc. A216, 547 (1953).

8. J. Bardeen, L. N. Cooper, and J. R. Schrieffer, Phys. Rev. 108, 1175 (1957).

9. L. W. Shubnikov, V. I. Khotkevich, J. D. Shepelev, and J. N. Rjabinin, Zh. Eksp. Teor. Fiz. 7, 221 (1937).

10. R. Radebaugh and P. H. Keesom, Phys. Rev. 149, 209, 217 (1966).

11. S. J. Williamson, Phys. Rev. B 2, 3545 (1970).

12. H. Rietschel and H. Winter, Phys. Rev. Lett. 43, 1256 (1979).

13. H. Rietschel, Phys. Rev. B 24, 155 (1981).

14. K. A. Gschneidner, Jr. and S. K. Dhar, Magnetic Excitations and Fluctuations (San Miniato, Italy, 1984), pp. 177-182.

15. K. A. Gschneidner, Jr., J. Magn. Magn. Mater. (to be published in 1985).

16. E. S. R. Gopal. Specific Heats at Low Temperatures (Plenum Press, New York, 1966).

17. K. Maki, Physics 1, 21 (1964).

18. W. H. Kleiner, L. M. Roth and S. H. Autler, Phys. Rev. A 133, 1226 (1964).

19. B. B. Goodman, Phys. Lett. 1, 215 (1962).

20. B. B. Goodman, IBM J. Res. Dev. 6, 63 (1962).

21. L. P. Gor'kov, Sov. Phys. JETP 10, 593 (1960).

22. R. R. Hake, Phys. Rev. 158, 356 (1967).

23. E. Fawcett, J. Phys. Chem. Solids 18, 320 (1961).

24. L. J. van der Pauw, Philips Research Reports 13, 1 (1958).

25. R. J. Stierman, Ph.D. thesis, Iowa State University, 1982 (unpublished).

26. J. R. Hopkins, Ph.D. thesis, Iowa State University, 1972 (unpublished).

27. Y.-C. S. Yeh, Ph.D. thesis, Iowa State University, 1984 (unpublished).

28. H. Padamsee, J. E. Neighbor and C. A. Shiffman, J. of Low Temp. Phys. 12, 387 (1973).

29. W. S. Corak, B. B. Goodman, C. B. Satterthwaite and A. Wexler, Phys. Rev. B 102, 656 (1956).

30. D. Shoenberg, Superconducting, 2nd ed. (Cambridge University Press, Cambridge, England, 1965).

31. B. B. Goodman, Compt. Rend. 246, 3031 (1958).

32. W. L. McMillan, Phys. Rev. 167, 331 (1968).

33. J. Zasadzinski, D. M. Burnell, E. L. Wolf and G. B. Arnold, Phys. Rev. B 25, 1622 (1982).

34. P. B. Allen and R. C. Dynes, Phys. Rev. B 12, 905 (1975).

35. K. Maki and T. Tsuzuki, Phys. Rev. A 139, 868 (1965).

36. T. McConville and B. Serin, Phys. Rev. A 140, 1169 (1965).

VII. ACKNOWLEDGMENTS

I would like to express my appreciation to Dr. Karl A. Gschneidner, Jr., my major professor, for suggesting the project, and for his patience, help and guidance during the research and throughout my graduate program. I am also indebted to Mr. Rick Schmidt for preparing the samples; to Dr. Sudesh Dhar and Mr. Jack Moorman for their assistance in taking the heat capacity data; to Mr. Jerry Ostenson and Mr. Peter Klavins for their constant sound advice and many helpful suggestions.

I would also like to thank my family and my dear friend, Chih-Ping; they have always been an encouragement to me through their love and understanding.

APPENDIX: MEASURED HEAT CAPACITY DATA

Measured Heat Capacity for Vanadium at H = 0.00 T

T (deg K)	C (mJ/gm-at deg K)	T (deg K)	C (mJ/gm-at deg K)
1.5012	2.9842730D+00	2.1244	1.2094770D+01
1.5296	3.3108818D+00	2.1725	1.3002297D+01
1.5565	3.4895790D+00	2.2206	1.3965351D+01
1.5832	3.8602307D+00	2.2523	1.4708943D+01
1.6100	4.0751360D+00	2.3009	1.5744616D+01
1.6348	4.4463342D+00	2.3499	1.6804272D+01
1.6597	4.7811221D+00	2.4025	1.7983262D+01
1.6829	4.9561281D+00	2.4582	1.9682085D+01
1.7072	5.1760251D+00	2.4974	2.0115253D+01
1.7292	5.5506170D+00	2.5614	2.1806438D+01
1.7438	5.5954821D+00	2.6250	2.3666901D+01
1.7586	5.8710809D+00	2.7352	2.6261131D+01
1.7839	5.7718829D+00	2.8143	2.8951508D+01
1.8081	6.6505049D+00	2.8938	3.0964574D+01
1.8347	7.0568145D+00	2.9729	3.4029372D+01
1.8551	7.4135733D+00	3.0574	3.6384808D+01
1.8831	7.8604757D+00	3.1223	3.8857136D+01
1.9201	8.4357372D+00	3.2084	4.0952050D+01
1.9609	8.9596309D+00	3.3029	4.5313879D+01
2.0008	9.7249700D+00	3.3961	4.6890870D+01
2.0304	1.0311605D+01	3.4127	4.8098700D+01
2.0787	1.1249759D+01	3.4419	4.9061616D+01

Measured Heat Capacity for Vanadium at H = 0.00 T (continued)

T (deg K)	C (mJ/gm-at deg K)	T (deg K)	C (mJ/gm-at deg K)
3.5183	5.1737257D+01	7.5471	9.3328611D+01
3.6208	5.5451095D+01	7.8199	9.8340790D+01
3.7374	6.0102944D+01	8.1251	1.0438893D+02
3.8547	6.4788180D+01	8.4282	1.0819699D+02
3.9426	6.7887590D+01	8.7426	1.1295432D+02
4.0559	7.2915788D+01	9.0683	1.2446814D+02
4.1723	7.8037834D+01	9.3774	1.2883198D+02
4.2954	8.3275188D+01	9.7266	1.4177973D+02
4.4206	8.8722740D+01	10.0958	1.4865154D+02
4.5399	9.4941433D+01	10.4561	1.4524795D+02
4.6816	1.0171694D+02	10.8278	1.6464875D+02
4.8237	1.0840826D+02	11.1639	1.7253147D+02
4.9725	1.1586260D+02	11.5293	1.7965665D+02
5.1231	1.2375250D+02	11.9561	1.8410764D+02
5.2594	1.3186682D+02	12.3955	1.9907662D+02
5.4548	8.3489876D+01	12.9108	2.2571864D+02
5.6792	6.4290125D+01	13.4004	2.3226534D+02
5.9225	6.8776436D+01	13.8397	2.6846700D+02
6.1738	7.3338429D+01	14.2997	2.6229542D+02
6.3873	7.4691577D+01	14.7405	2.6607284D+02
6.6621	7.8932280D+01	15.1989	2.9212614D+02
6.9534	8.3074848D+01	15.6459	3.0826784D+02
7.2511	8.7701043D+01	16.1291	3.4082392D+02

Measured Heat Capacity for Vanadium at H = 0.00 T (continued)

T (deg K)	C (mJ/gm-at deg K)	T (deg K)	C (mJ/gm-at deg K)
16.6346	3.4100625D+02	18.6555	4.5249408D+02
17.0980	4.3629468D+02	19.2920	4.8958533D+02
17.6429	4.6650848D+02	19.9327	5.5618055D+02
18.1659	4.3408563D+02		

Measured Heat Capacity for Vanadium at H = 1.25 T

T (deg K)	C (mJ/gm-at deg K)	T (deg K)	C (mJ/gm-at deg K)
1.5662	1.5660868D+01	1.9064	1.8461214D+01
1.5822	1.6007175D+01	1.9347	1.8752679D+01
1.5988	1.6296530D+01	1.9657	1.9112037D+01
1.6187	1.5745627D+01	1.9979	1.9347453D+01
1.6305	1.5189009D+01	2.0322	1.9883456D+01
1.6663	1.7269810D+01	2.0720	2.0017242D+01
1.6850	1.5738689D+01	2.1103	2.0709916D+01
1.7059	1.6783297D+01	2.1510	2.0838485D+01
1.7266	1.7140855D+01	2.1945	2.1357391D+01
1.7468	1.7176057D+01	2.2416	2.2190076D+01
1.7789	1.7208640D+01	2.2901	2.2758708D+01
1.8022	1.7399719D+01	2.3439	2.3361090D+01
1.8275	1.7469651D+01	2.4034	2.3801371D+01
1.8512	1.8124747D+01	2.4619	2.4567113D+01
1.8750	1.8268991D+01	2.5793	2.6284645D+01

Measured Heat Capacity for Vanadium at H = 125 T (continued)

T (deg K)	C (mJ/gm-at deg K)	T (deg K)	C (mJ/gm-at deg K)
2.6486	2.7301374D+01	5.1889	5.7825480D+01
2.7230	2.7807437D+01	5.2833	6.0327736D+01
2.8829	2.9739961D+01	5.3322	6.0205347D+01
2.9509	3.0877988D+01	5.3495	5.9179106D+01
3.0420	3.1619212D+01	5.4250	6.0617214D+01
3.1362	3.2739148D+01	5.4982	6.1541101D+01
3.2354	3.3980319D+01	5.5406	6.2732390D+01
3.3385	3.5609856D+01	5.5641	6.3362265D+01
3.3594	3.5234856D+01	5.6283	6.5318775D+01
3.4298	3.6012012D+01	5.6986	6.5633325D+01
3.4919	3.6848926D+01	5.7365	6.5703656D+01
3.6184	3.8176091D+01	5.7696	6.4431801D+01
3.7535	3.9642153D+01	5.8454	6.7770782D+01
3.8842	4.0669561D+01	5.9233	6.8578993D+01
4.0470	4.2997351D+01	5.9550	6.8372990D+01
4.2151	4.5348401D+01	6.0127	6.8413117D+01
4.3898	4.7405441D+01	6.1081	7.0558880D+01
4.5739	4.9620438D+01	6.1819	7.2042402D+01
4.7427	5.1414421D+01	6.2080	7.3098328D+01
4.9364	5.3410083D+01	6.3153	7.3710562D+01
5.1098	5.5745053D+01	6.4187	7.5020670D+01
5.1324	5.7334062D+01	6.5398	7.6985229D+01

Measured Heat Capacity for Vanadium at H = 1.25 T (continued)

T (deg K)	C (mJ/gm-at deg K)	T (deg K)	C (mJ/gm-at deg K)
6.6661	7.9833484D+01	11.8251	1.8254490D+02
6.8014	8.1760704D+01	12.2163	1.9022631D+02
6.9407	8.3835978D+01	12.6396	2.0402269D+02
7.0732	8.5456780D+01	13.0542	1.9098623D+02
7.2227	8.8033076D+01	13.4339	2.2354839D+02
7.3814	9.1128777D+01	13.8295	2.6295703D+02
7.5485	9.3709583D+01	14.2331	2.5511083D+02
7.7253	9.7134323D+01	14.6698	2.6877339D+02
7.9156	9.9040315D+01	15.1164	2.7795964D+02
8.1486	1.0377929D+02	15.5531	3.0578539D+02
8.3859	1.0760134D+02	15.9941	2.9687332D+02
8.6288	1.1278650D+02	16.4138	3.4362152D+02
8.8827	1.1626695D+02	16.8778	3.9910506D+02
9.1209	1.1994235D+02	17.3317	3.7865379D+02
9.3955	1.2917694D+02	17.7835	3.8984878D+02
9.6745	1.2983549D+02	18.2519	4.3674773D+02
9.9660	1.3813616D+02	18.7677	5.1411368D+02
10.2590	1.4263221D+02	19.5166	4.8293347D+02
10.5343	1.5230030D+02	20.2158	4.4807883D+02
10.8632	1.5782653D+02	20.8030	4.1241888D+02
11.2035	1.6247492D+02		
11.5126	1.6769263D+02		

Measured Heat Capacity for Vanadium at H = 2.50 T

T (deg K)	C (mJ/gm-at deg K)	T (deg K)	C (mJ/gm-at deg K)
1.4438	1.5022156D+01	1.9647	1.9735313D+01
1.4646	1.5779569D+01	2.0115	2.0279029D+01
1.4749	1.4771501D+01	2.0570	2.0787202D+01
1.4863	1.4817436D+01	2.1099	2.1721314D+01
1.4984	1.5245979D+01	2.1649	2.1835251D+01
1.5175	1.6492459D+01	2.2237	2.2420051D+01
1.5301	1.6592719D+01	2.2884	2.2932437D+01
1.5431	1.6480202D+01	2.3507	2.3209690D+01
1.5567	1.6230271D+01	2.4193	2.4202626D+01
1.5713	1.6151595D+01	2.4920	2.4775021D+01
1.5919	1.6754796D+01	2.5737	2.5958197D+01
1.6088	1.7098101D+01	2.6609	2.6880728D+01
1.6268	1.7144992D+01	2.7450	2.7894081D+01
1.6455	1.6963516D+01	2.8441	2.9129449D+01
1.6657	1.7095962D+01	2.9471	2.9982492D+01
1.6934	1.7045613D+01	3.0514	3.1382891D+01
1.7173	1.7241143D+01	3.1608	3.2992530D+01
1.7446	1.7693520D+01	3.2618	3.4038515D+01
1.7740	1.8338978D+01	3.3835	3.5064755D+01
1.8061	1.8485057D+01	3.5049	3.6724666D+01
1.8391	1.8977162D+01	3.6154	3.7839539D+01
1.8785	1.9196331D+01	3.7349	3.9365749D+01
1.9206	1.9305316D+01	3.8825	4.0941214D+01

Measured Heat Capacity for Vanadium at H = 2.50 T (continued)

T (deg K)	C (mJ/gm-at deg K)	T (deg K)	C (mJ/gm-at deg K)
4.0361	4.2821128D+01	9.1475	1.2736842D+02
4.1897	4.4700716D+01	9.4711	1.3165711D+02
4.2353	4.5397738D+01	9.8024	1.3810467D+02
4.3554	4.6810806D+01	10.1352	1.4502941D+02
4.4168	4.7655318D+01	10.4749	1.5368982D+02
4.6222	5.0048200D+01	10.7977	1.6520164D+02
4.8295	5.2741927D+01	11.1446	1.7285636D+02
5.0398	5.7907391D+01	11.4697	1.7856669D+02
5.2279	5.9168147D+01	11.7899	1.8603263D+02
5.4458	6.1932332D+01	12.1263	2.0399395D+02
5.6729	6.5567112D+01	12.4688	2.0593800D+02
5.9108	6.8310219D+01	12.8460	2.1854047D+02
6.1464	7.1879598D+01	13.2352	2.2622338D+02
6.3594	7.5341065D+01	13.6384	2.2895831D+02
6.6078	7.9836597D+01	14.0600	2.4602966D+02
6.8665	8.2883909D+01	14.4738	2.7235964D+02
7.1311	8.8225594D+01	14.9292	2.9295505D+02
7.4046	9.4966133D+01	15.383	3.2027678D+02
7.6744	9.7239223D+01	15.8545	3.5232244D+02
7.9701	1.0300253D+02	16.3369	3.5294234D+02
8.2643	1.0915256D+02	16.7944	3.8712293D+02
8.5554	1.1421941D+02	17.2552	3.7985478D+02
8.8601	1.2021718D+02	17.7421	3.9834281D+02

Measured Heat Capacity for Vanadium at H = 2.50 T (continued)

T (deg K)	C (mJ/gm-at deg K)	T (deg K)	C (mJ/gm-at deg K)
18.2773	4.1981816D+02	20.5020	5.4021496D+02
18.8280	4.3615970D+02	21.1148	6.0122571D+02
19.3644	4.9041330D+02	21.6935	6.4245824D+02
19.9063	5.3173450D+02		

Measured Heat Capacity for Vanadium at H = 5.39 T

T (deg K)	C (mJ/gm-at deg K)	T (deg K)	C (mJ/gm-at deg K)
1.5337	1.5604466D+01	1.7563	1.7880430D+01
1.5427	1.5763909D+01	1.7842	1.8020243D+01
1.5526	1.5767220D+01	1.8156	1.8570519D+01
1.5627	1.6289447D+01	1.8513	1.8551444D+01
1.5738	1.6165195D+01	1.8893	1.9007118D+01
1.5860	1.6574988D+01	1.9235	1.9461637D+01
1.5984	1.6624436D+01	1.9676	1.9738570D+01
1.6112	1.6422866D+01	2.0147	2.0227672D+01
1.6250	1.6967728D+01	2.0630	2.0684445D+01
1.6401	1.7000654D+01	2.1139	2.1210097D+01
1.6542	1.7178837D+01	2.2566	2.2486815D+01
1.6714	1.7266132D+01	2.3118	2.3102303D+01
1.6897	1.7007459D+01	2.4461	2.4495175D+01
1.7110	1.7480275D+01	2.5230	2.5055990D+01
1.7349	1.7625712D+01	2.6007	2.6068027D+01

Measured Heat Capacity for Vanadium at H = 5.39 T (continued)

T (deg K)	C (mJ/gm-at deg K)	T (deg K)	C (mJ/gm-at deg K)
2.6846	2.7119755D+01	6.0900	6.9617307D+01
2.7758	2.8042656D+01	6.2330	7.1438866D+01
2.8634	2.9038917D+01	6.4097	7.4426195D+01
2.9584	3.0075450D+01	6.5941	7.7365212D+01
3.0301	3.0737929D+01	6.7804	8.0117113D+01
3.1325	3.1836157D+01	6.9711	8.2618297D+01
3.2415	3.3256856D+01	7.1344	8.5465423D+01
3.3576	3.4335641D+01	7.3674	8.9258272D+01
3.4785	3.6022127D+01	7.5986	9.1835480D+01
3.5778	3.7264849D+01	7.8294	9.7257415D+01
3.7032	3.8568235D+01	8.0762	1.0062630D+02
3.8350	4.0104722D+01	8.2931	1.0515005D+02
3.9761	4.2114588D+01	8.5653	1.1013348D+02
4.1420	4.2803171D+01	8.8492	1.1419333D+02
4.8389	5.2614574D+01	9.1297	1.1942879D+02
4.9750	5.3877605D+01	9.4251	1.2438591D+02
5.1109	5.5845185D+01	9.7013	1.3473635D+02
5.2456	5.6408089D+01	10.0130	1.3983347D+02
5.3790	5.9148847D+01	10.3408	1.4781416D+02
5.4976	6.1203789D+01	10.6778	1.5408904D+02
5.6493	6.3293657D+01	11.0252	1.6481632D+02
5.7931	6.5277461D+01	11.3237	1.7290037D+02
5.9341	6.7311390D+01	11.6632	1.8190901D+02

Measured Heat Capacity for Vanadium at H = 5.39 T (continued)

T (deg K)	C (mJ/gm-at deg K)	T (deg K)	C (mJ/gm-at deg K)
12.0213	1.8373596D+02	15.8243	3.0464401D+02
12.3898	1.9813737D+02	16.3215	3.7627059D+02
12.7790	2.1793250D+02	16.8272	3.3563538D+02
13.1690	2.1592115D+02	17.3354	3.7734546D+02
13.5907	2.4897161D+02	17.8356	3.9371508D+02
14.0373	2.3959398D+02	18.3802	4.4737971D+02
14.4639	2.5027134D+02	18.9537	4.7224732D+02
14.8956	2.7273905D+02	19.5296	4.7711189D+02
15.3423	2.5987202D+02	20.1212	6.1538943D+02

Measured Heat Capacity for Vanadium at H = 7.62 T

T (deg K)	C (mJ/gm-at deg K)	T (deg K)	C (mJ/gm-at deg K)
1.4860	1.4472468D+01	1.6087	1.6408648D+01
1.4989	1.4842213D+01	1.6257	1.6421087D+01
1.5100	1.5048999D+01	1.6466	1.6564283D+01
1.5199	1.5198905D+01	1.6703	1.6937193D+01
1.5303	1.5220862D+01	1.6957	1.7100206D+01
1.5421	1.5594855D+01	1.7204	1.7371817D+01
1.5538	1.5726611D+01	1.7481	1.7583825D+01
1.5664	1.5905562D+01	1.7803	1.7879322D+01
1.5798	1.6118070D+01	1.8163	1.8158403D+01
1.5943	1.6139649D+01	1.8562	1.8666750D+01

Measured Heat Capacity for Vanadium at H = 7.62 T (continued)

T (deg K)	C (mJ/gm-at deg K)	T (deg K)	C (mJ/gm-at deg K)
1.8942	1.8665472D+01	3.9391	4.1107350D+01
1.9414	1.9153835D+01	4.0834	4.2843536D+01
1.9925	1.9675855D+01	4.2053	4.4691367D+01
2.0463	2.0188847D+01	3.4709	4.6877969D+01
2.1038	2.0755440D+01	3.5386	4.8273849D+01
2.1784	2.1578146D+01	4.6974	5.1443464D+01
2.2337	2.2050514D+01	3.8705	5.2077350D+01
2.2969	2.2558105D+01	5.0068	5.3277453D+01
2.3633	2.3336376D+01	5.1956	5.6435183D+01
2.4459	2.4199883D+01	5.3910	5.9070600D+01
2.5210	2.5063685D+01	5.5888	6.2155052D+01
2.6576	2.6620995D+01	5.7960	6.4850618D+01
2.7424	2.7792077D+01	5.9717	6.7885024D+01
2.8348	2.8811526D+01	6.1923	7.0720479D+01
2.9295	2.9609163D+01	6.4103	7.4029041D+01
3.0037	3.0560527D+01	6.6427	7.7316508D+01
3.1069	3.1894331D+01	6.8890	8.0718156D+01
3.2173	3.3269137D+01	7.1190	8.4276684D+01
3.3313	3.4547898D+01	7.3876	8.9086417D+01
3.4479	3.5840398D+01	7.6821	9.3856902D+01
3.5715	3.7255731D+01	7.9817	9.9311877D+01
3.6667	3.8075278D+01	8.2689	1.0579634D+02
3.7975	3.9493727D+01	8.5206	1.0876160D+02

Measured Heat Capacity for Vanadium at H = 7.62 T (continued)

T (deg K)	C (mJ/gm-at deg K)	T (deg K)	C (mJ/gm-at deg K)
8.8342	1.1641323D+02	13.9154	2.4701357D+02
9.1460	1.2223905D+02	14.3287	2.5065328D+02
9.4477	1.2674310D+02	14.7542	2.5307073D+02
9.7506	1.3314833D+02	15.1880	2.7836836D+02
10.0317	1.3813192D+02	15.6231	3.0871399D+02
10.3477	1.4719596D+02	16.1032	3.0368154D+02
10.6725	1.5357021D+02	16.5961	3.3692402D+02
11.0110	1.6203741D+02	17.0772	3.5083091D+02
11.3391	1.6944866D+02	17.5607	3.7883932D+02
11.6413	1.7568640D+02	18.0402	3.7920181D+02
11.9854	1.8519485D+02	18.5504	4.0249719D+02
12.3726	1.9377084D+02	19.0685	4.6388530D+02
12.7782	1.9328520D+02	19.5995	5.3956761D+02
13.1582	2.1847489D+02	20.1404	4.6103392D+02
13.5188	2.1644422D+02	20.6623	4.6973163D+02

Measured Heat Capacity for Vanadium at H = 9.98 T

T (deg K)	C (mJ/gm-at deg K)	T (deg K)	C (mJ/gm-at deg K)
1.7421	1.7301084D+01	1.7821	1.8034623D+01
1.7534	1.7452337D+01	1.7942	1.8017652D+01
1.7625	1.7621190D+01	1.8056	1.8289359D+01
1.7719	1.7715860D+01	1.8176	1.8165463D+01

Measured Heat Capacity for Vanadium at H = 9.98 T (continued)

T (deg K)	C (mJ/gm-at deg K)	T (deg K)	C (mJ/gm-at deg K)
1.8305	1.8217356D+01	2.5950	2.5723591D+01
1.8445	1.8536848D+01	2.6625	2.6595770D+01
1.8584	1.8720349D+01	2.7328	2.7280121D+01
1.8737	1.8894382D+01	2.8109	2.8239759D+01
1.8907	1.8892884D+01	2.8771	2.9016332D+01
1.9109	1.6738813D+01	2.9646	2.9986521D+01
1.9316	2.2010222D+01	3.0524	3.0922664D+01
1.9502	1.9553793D+01	3.1473	3.1884732D+01
1.9750	1.9714736D+01	3.2450	3.3216210D+01
2.0018	2.0056466D+01	3.3301	3.4247333D+01
2.0315	2.0265519D+01	3.4373	3.5338532D+01
2.0639	2.0528383D+01	3.5482	3.6443333D+01
2.0926	2.0859871D+01	3.6640	3.8382336D+01
2.1294	2.1069958D+01	3.7854	3.9274588D+01
2.1682	2.1462196D+01	3.8966	4.0397317D+01
2.2096	2.1918520D+01	4.0274	4.2194365D+01
2.2549	2.2330477D+01	4.1684	4.3913004D+01
2.2859	2.2621252D+01	4.3198	4.5967427D+01
2.3308	2.3131016D+01	4.4781	4.7618396D+01
2.3777	2.3324374D+01	4.6079	5.0473930D+01
2.4281	2.3878360D+01	4.7740	5.1703481D+01
2.4839	2.4422634D+01	4.9451	5.4681653D+01
2.5323	2.4929459D+01	5.1289	5.6629338D+01

Measured Heat Capacity for Vanadium at H = 9.98 T (continued)

T (deg K)	C (mJ/gm-at deg K)	T (deg K)	C (mJ/gm-at deg K)
5.3134	5.7674328D+01	11.2882	1.7052401D+02
5.4516	6.0275841D+01	11.6766	1.8095001D+02
5.6544	6.2952865D+01	12.0778	1.9408762D+02
5.8652	6.6153875D+01	12.4964	1.9707068D+02
6.0832	6.9227131D+01	12.9267	2.0765402D+02
6.3028	7.4337131D+01	13.3519	2.2887605D+02
6.5259	7.0701884D+01	13.7908	2.4613052D+02
6.7230	7.8561843D+01	14.2266	2.4567409D+02
7.0081	8.3511181D+01	14.6711	2.8930160D+02
7.2935	8.8535549D+01	15.1435	3.0122418D+02
7.5865	9.3114646D+01	15.5795	3.2853393D+02
7.8727	9.8234577D+01	16.0632	2.8849101D+02
8.1914	1.0433778D+02	16.5590	3.6950471D+02
8.5044	1.1010466D+02	17.0481	4.1204029D+02
8.8231	1.1654847D+02	17.5353	3.8654803D+02
9.1457	1.2241115D+02	18.0913	4.3415751D+02
9.4527	1.2987852D+02	18.6983	4.7441860D+02
9.8035	1.3749909D+02	19.2319	6.0594582D+02
10.1782	1.4611712D+02	19.8332	4.8377117D+02
10.5742	1.5390373D+02	20.3833	5.6887350D+02
10.9472	1.6361486D+02		